MODELING THE EVOLUTION OF SUBSTRATE USE IN THE HANDS AND FEET OF PRIMATES, BIRDS, AND NON-AVIAN THEROPOD DINOSAURS

by

Josef Barrett Stiegler

A thesis submitted in partial fulfillment
of the requirements for the degree

of

Master of Science

in

Earth Sciences

MONTANA STATE UNIVERSITY
Bozeman, Montana

May, 2012

APPROVAL

of a thesis submitted by

Josef Barrett Stiegler

This thesis has been read by each member of the thesis committee and has been found to be satisfactory regarding content, English usage, format, citation, bibliographic style, and consistency, and is ready for submission to The Graduate School.

Dr. David J. Varricchio

Approved for the Department of Earth Sciences

Dr. David Mogk

Approved for The Graduate School

Dr. Carl A. Fox

STATEMENT OF PERMISSION TO USE

Josef Barrett Stiegler

May 2012

ACKNOWLEDGEMENTS

First I would like to thank my committee members David Varricchio, Jack Horner, and David Willey for their support throughout my time at Montana State and guidance on this project. This work was greatly improved by unpublished data kindly contributed by Mark Hamrick, Pierre Lemelin, and Jonah Choiniere. I am thankful for the assistance of numerous students, staff, and curators at the MOR, RTMP, AMNH, NMNH, LSUMNS, IVPP, and DNHM. I would like to thank Annliv Young and family, Will Miller and family, Colin McNamara, Bart Huber, Curtis Ramsey, Judd Meyer, Miceh Cumpian, and Daniel Holman for providing housing while I travelled for work related to this project, and Ed Kronfuss for providing a vehicle. I thank The Paleontological Society, the Society of Vertebrate Paleontology, David Varricchio, and the Departments of Earth Sciences and Biological Sciences for providing funding for this project. Numerous graduate and undergraduate students at MSU provided helpful comments and moral support. In alphabetical order I would specifically like to thank Ash, Ben, Beth, Bobby, Bryan A., Bryan T., Cathy, Darrin, Denver, Evan, John, Josh, Justin, Kelsey, Liz, Mike, Robert, Ryan, Sarah, Scott, Syverine, Tara, Todd, Tom, and Trish. The Bozeman Cutthroat Rugby Club treated me like a brother from the time I arrived in Montana to the time I left, and for that I am forever grateful. Finally, I thank my family for always loving and encouraging me in school and in life. Mom, Dad, Ben, and Daniel, you guys are the best.

TABLE OF CONTENTS

LIST OF TABLES

Table Page

LIST OF FIGURES

Figure Page

ABSTRACT

The hands and feet of non-avian theropods have historically been characterized as structures adapted for grasping prey items and for cursorial locomotion, respectively. The purpose of this study was to challenge those assumptions in light of observations on the intradigital proportions of the hands and feet of theropods compared to modern taxa. Linear measurements of elements from the hands of mammals and squamates, the feet of birds, and both the hands and feet of non-avian theropods were collected to observe clustering of taxa in morphospace. The evolution of each linear character was modeled for primates, birds, and non-avian theropods using Ornstein-Uhlenbeck models in the "OUCH!" software package. Brownian motion models were nearly universally rejected in favor of single and multi-optimum selection based models. Model testing indicated directional selection for the most proximal and distal non-ungual elements in each digital ray, and either stabilizing selection or brownian motion processes for intermediate elements. The results for models applied to non-avian theropods suggest selection for metacarpal proportions convergent with arboreal mammals, and proportions of the penultimate phalanx similar to the feet of birds that use clawed adhesion for vertical substrate use and predation. We propose that "clinging" as opposed to "grasping" is a more apt hypothesis for behavior leading to elongation of the penultimate phalanx, as is the case in most non-avian theropods. According to modeling results, microraptorine dromaeosaurids evolved proportionally long metacarpals relative to their manual phalanges convergently with birds, and were comparable to other non-avian theropods in pedal proportions. These results contradict previous hypotheses in the literature regarding arboreal substrate use within microraptorinae. The scansoriopterygid *Epidendrosaurus* was a slight outlier in both manual and pedal proportions from other non-avian maniraptorans, but adaptation for an arboreal lifestyle in this taxon is not supported by this analysis. The "Raptor Prey Restraint" model for predatory behavior in deinonychosaurian theropods was rejected by this analysis, though it is likely that the evaluated traits fail to capture the necessary anatomical variation to more fully test this hypothesis.

INTRODUCTION

The manual and pedal phalanges of vertebrates are under constant selection due to their regular contact with substrates, and therefore should be the most prone to convergence of any appendicular element, whether terrestrial, arboreal, aqueous, or even prey items. Accordingly, many authors have attempted to reconstruct the behavior of extinct organisms through the analysis of phalangeal measurements. One commonly employed method is to view the elements of a three-component system in ternary space and assess the proximity of fossil taxa to clusters of modern organisms related by a common behavior (e.g. Hopson, 2001; Hamrick, 2001; Kirk et al., 2008; Fröbisch and Reisz, 2009; Morchauser et al., 2009). This is a useful way to visualize the data and test for a general convergent pattern, but it does little to test functional hypotheses quantitatively, nor does it account for the effects of phylogeny on trait evolution.

Since Felsenstein's phylogenetically independent contrasts (Felsenstein, 1985) and Grafen's phylogenetic regression (Grafen, 1989) were introduced for the modeling of continuous morphological characters, phylogenetic comparative methods have generally assumed that characters evolved by Brownian motion (BM) (Ricklefs and Starck, 1996; Carvalho et al. 2006, Pyenson and Sponberg, 2011). Because closely related species are more likely to be similar for any particular trait than distantly related species, ordinary statistical methods (i.e. least squares regression) that treat the data as if they are independent and identically distributed are insufficient (Maddison, 2000). The application of a BM model to data distributed across a phylogeny assumes an element of

"random walk" for the trait in question that is independent along each branch. Under these models, the trait is allowed to vary following each cladogenetic event (at each node). BM is advantageous as an evolutionary model in a statistical context because it produces a normal distribution of character states. Felsenstein himself, however, acknowledged two cases in which BM would be inappropriate: (1) when selection is continuous across speciation events or during anagenesis such that trait changes are correlated through time, and (2) when multiple lineages experience similar selective pressures due to similar environmental conditions, food type, predators, etc. (Felsenstein, 1985). As comparative phylogenetic studies have demonstrated, both of these conditions are often met for adaptive scenarios involving locomotor characters or limbs in contact with substrates (Salton and Szalay, 2004; Sanchez and Berta, 2010; Nyakatura and Fischer, 2011; Smith, 2011). Therefore, models that use BM to model evolution for these types of characters make false assumptions and models that incorporate phylogeny and selection are necessary.

Hansen (1997) proposed a simple model for continuous traits evolving under selection based on the Ornstein-Uhlenbeck (OU) process of particle physics that describes the effect of friction on a Brownian particle. Butler and King (2004) adapted this model in their software package "OUCH!", and these models have previously been applied to such varied systems as the evolution of body size in island dwelling *Anolis*, piscivory in centrarchid fishes, and genome size in angiosperms (Pinto et al., 2008; Collar et al., 2009; Beaulieu et al., 2010).

The simplest version of the model (Equation 1) has two terms, and describes the change in a trait through time ($dX(t)$).

Equation 1. $$dX(t) = \alpha[\theta - X(t)]dt + \sigma dB(t)$$

The first term denotes the change of the trait with respect to an adaptive peak or evolutionary optimum (θ) through time, and the relative strength of selection acting on that trait (α). The second term describes the change of the trait due to genetic drift ($dB(t)$) and the relative strength of drift acting on the trait (σ). When the strength of selection (α) equals zero the model reverts to Brownian motion (Equation 2).

Equation 2. $$dX(t) = \sigma dB(t).$$

The function of non-avian theropod hands and feet are an interesting test case for these models. Despite widely disparate morphologies, there is a persistent assumption in the literature that the hands of most predatory theropods functioned in grasping prey, and/ or that a morphology suggestive of grasping behavior is the ancestral condition for the group (Ostrom, 1969; Colbert, 1989; Sereno,1993, 1999; Zanno, 2006). In addition, new hypotheses regarding foot use in mesozoic theropods have challenged old ideas about predatory behavior and the origins of flight (Kambic, 2008; Fowler et al., 2011).

The manual unguals of many theropods are highly recurved (especially in Deinonychosauria), and many possess elongate penultimate phalanges within each digit. A similar pattern is seen in the feet of raptorial birds, and in light of these observations, the hands of non-avian theropods have long been attributed grasping functions (Lambe, 1904; Osborn, 1916; Gilmore, 1920; Madsen, 1976; Sereno,1993,1999; Hopson, 2001;

Xu et al. 2009, among many others). This has led some to suggest that these "grasping" hands were exapted for use in climbing (Naish, 2000; Witmer, 2002; Chatterjee and Templin, 2004), while others questioned if perhaps the predatory "grasping" motions of theropods were the precursors to the flight stroke (Gauthier and Padian, 1985; Gishlick, 2001). A recent study suggested that the feet of accippitrid raptors are optimized not only for grasping, but for clinging to large prey items (Fowler et al., 2009). This is an important distinction because while grasping, a hand or foot contacts the substrate loaded primarily in compression with all phalanges flexed, as in the feet of perching birds or the hands of arboreal primates and creates forces normal to the surface of the grasped object (Hildebrand, 2001). While clinging, a hand or foot contacts the substrate with the phalanges loaded in tension (Boyer and Bloch, 2008). Clinging behaviors most often involve adhesion to the substrate using non-frictional grip mechanisms which include dry adhesion, suction, or interlocking with claws (Cartmill, 1985, Hildebrand, 2001). Clawed clinging generally occurs with the non-ungual phalanges in an extended position (or at least not fully flexed) as in the hands and feet of a squirrel climbing a tree (Boyer and Bloch, 2008). These definitions underline the importance of specificity when hypothesizing behaviors for extinct organisms.

There have been limited mentions of theropod feet as grasping structures as well (Madsen, 1976; Varricchio, 2001), but they are generally referred to in a locomotor context as organs of cursorial locomotion due to their apparently hinge-like mesotarsal ankle joints. Additionally, some argue that small maniraptorans may have been arboreal,

necessitating a climbing function for both the hands and feet (Zhang, 2002). On the heels of their observations for modern raptors, Fowler et al. (2009, 2011) proposed that the feet of some advanced coelurosaurs functioned in prey restraint, arguing for a grasping function in the foot of *Deinonychus.*

These characterizations have come from comparisons of theropod hands and feet to the feet of birds. While making these comparisons may bear fruitful observations, an analogy to unrelated organisms provides a different kind of test. Contradicting the assumption by theropod researchers, Hamrick (2001) suggests that in mammals, elongate proximal phalanges and not penultimate phalanges are suggestive of grasping function. The hands of primates are universally used as grasping organs regardless of locomotor mode (Cartmill, 1992; Bloch and Boyer, 2002); therefore, a functional signal related to grasping in the intradigital proportions of primates should reflect the tendency of use of the hand in prehension relative to pronograde or orthograde locomotor postures.

The purpose of this study was to test the efficacy of OU models for describing trait evolution in the hands and feet of taxa with known behaviors related to substrate-use, and apply similar models to the evolution of the same characters in mesozoic theropods. In doing so we challenge previous assumptions about the grasping and cursorial functions of theropod hands and feet, respectively. We estimated phylogenies for primates as well as mesozoic and extant theropods and used the topologies to investigate the evolution of manual and pedal digital ray proportions using selection-based models in OUCH! By taking a modeling approach that incorporates selection,

drift, and phylogeny, we more realistically estimated character evolution than would be possible using only BM models.

METHODS

Phylogenetic Analyses

The sequence alignments of Hackett et al. (2008) and Perelman et al. (2011) were used to estimate the phylogenies of extant birds and primates, respectively. The bird dataset consisted of 171 taxa representing all but three non-passerine families, all major passerine clades, and two crocodilian outgroups with sequences from 19 nuclear loci. (Hackett et al. 2008). The primate dataset consisted of 186 primate species representing all families, as well five non-primate euarchontogliran outgroup taxa with sequences from 54 nuclear loci. Maximum likelihood tree searches were conducted on the Cipres Science Gateway TeraGrid using RAxML. Each gene received its own partition, and each protein coding gene was partitioned by codon position. All partitions received the GTR+Gamma model of nucleotide substitution with 25 distinct rate categories. Estimation of mesozoic theropod phylogeny was conducted using a previously described, but unpublished matrix (Choiniere et al., 2010) consisting of 130 taxa and 555 discrete, unordered characters using parsimony in TNT (Goloboff et al., 2003). The matrix includes 92 coelurosaurian theropods (including 5 mesozoic bird taxa) along with 36 additional taxa such as basal tetanurans, ceratosaurs, and coelophysoids, as well as the outgroup taxa *Plateosaurus* and *Eoraptor*. The heuristic search had a simple addition sequence, held 2 trees at each step, and branch swapping was by tree bisection-

reconnection. Taxa that were missing from the continuous character data set were pruned from the recovered most-parsimonious trees.

Continuous Character Data Collection

Length measurements were collected for elements of the central digital ray in primate hands, bird feet, and the hands and feet of mesozoic theropods. Taxa were selected for study based on behavioral categories, availability in museum collections or in the literature, and their inclusion in recent phylogenetic analyses.

For the primate data set, measurements from the hands of 72 primate species and four outgroup taxa were collected directly from museum specimens and additional data for some species were taken from Kirk et al. (2008). 54 of the original 61 primate genera in the sequence alignment are represented in the measurements. For the extant bird data set, measurements from 79 species were taken directly from museum specimens and 48 were retrieved from a previous study (Hopson, 2001). 127 of the 171 in the bird sequence alignment are represented. For theropod hands, measurements were collected for 63 specimens representing 44 genera. Of these genera, three were basal birds, meaning Mesozoic, non-ornithurine avialans. Measurements for 16 specimens were collected personally and the remaining measurements were collected from the literature. For theropod feet, measurements were collected for 65 specimens representing 42 genera including 37 non-avian theropods and 5 basal birds 21 specimens were collected personally and the remaining data was collected from the literature. Both mesozoic

theropod samples are unfortunately dominated by coelurosaurs due to the poor record of complete hands and feet for ceratosaurs and basal tetanurans. However, there are sufficient non-coelurosaurs present to polarize the ancestral character conditions.

In primate and non-avian theropod hands, maximum length measurements were taken from the central metacarpal and each of its corresponding non-ungual phalanges, and converted to a percentage of the total length of the digital ray. For primates this is the third digit, and for non-avian theropods it is the second (although see Xu et al. 2009 for a differing opinion on the homology of theropod digits). In some cases, deep trochleation of phalangeal articular surfaces caused overlap in the total lengths of phalanges across an interphalangeal joint. To avoid biasing measurements when articular surfaces were deeply trochleated, measurements were taken from the distal aspect of the proximal articular end of each phalanx to the most distal aspect of the distal trochlear surface of each phalanx. While we anticipate that the effect of taking total lengths in these cases would be minor, the experimental design was to assess the functional lengths of intradigital elements, so this protocol improves the accuracy of our experiments and interpretations. We encourage future researchers to make this distinction when reporting phalangeal measurements. In cases where measurements were collected from multiple specimens of the same taxon, the measurements were first converted to percentages and then the means of those component percentages were used for further data analysis. We will hereafter refer to the proximal, intermediate and distal element in the examined three component systems as

mPE% (manual proximal element %), mIE% (manual intermediate element %), and mDE % (manual distal element %) in the manus, respectively; and pPE% (pedal proximal element %), pIE% (pedal intermediate element %), and pDE% (pedal distal element %) in the pes, respectively.

Along with the present data set, a larger collection of measurements was compiled for other extant tetrapods . The larger manual intradigital data set consisted of 705 sets of measurements from 260 mammalian species in addition to the previously discussed primate dataset and 85 sets of measurements from 49 reptile species. Measurements were taken from the second digital ray of reptile hands for consistency in element patterning. Mammalian groups present in this larger data set include monotremes, didelphimorph, dasyuromorph, paramelemorph, and diprotodontian marsupials; and, all major radiations of terrestrial eutherians including both bipedal and quadrupedal forms. Bipedal groups represented included dipodid and pedetid rodents, macropodiform marsupials, and *Homo sapiens*. Reptilian groups present in the data set include turtles and crocodilians as well as iguanian, gekkotan, scincomorph, and varanid lizards. The larger pedal intradigital data set consisted of measurements from 71 additional avian taxa with particular emphasis given to sampling accipitrid raptors, woodpeckers, and woodcreepers due to the underrepresentation of these groups in the phylogenetic data set.

The total data sets were plotted in ternary morphospace for qualitative observation of behavioral clustering. The taxa present in the supplementary data sets were not

included in the modeling analyses for this study due to the unavailability of densely taxonomically sampled and well-resolved molecular phylogenies in the case of the mammalian and reptilian groups, and their exclusion from the phylogenetic analysis of Hackett et al. (2008) in the case of the additional birds.

Model Definitions and Hypotheses

Four different sets of models were tested for the evolution of continuous characters: one set each for the hands of primates, the feet of birds, the hands of mesozoic theropods, and the feet of mesozoic theropods. The first two models in each set (BM and an OU model with a single optimum) are simple and require no behavioral information. For the remaining models, the taxa and their terminal branches were assigned to various iterations of behavioral optima for their hands and feet based on published behavioral accounts in the case of extant taxa, and hypotheses for Mesozoic taxa, some of which were based on our qualitative observation of the data while others were taken from the literature. Primate behavioral data primarily followed Fleagle (1999), Nowak (1999), and Youlatos and Meldrum (2011); and bird behavioral data primarily followed Harrison and Greensmith (1993), Hopson (2001), and Elphick et al. (eds.) (2001). Behavioral definitions are listed in Table 1. In some models, behaviors were combined into a single optimum, i.e. arboreal grasping and vertical clinging behaviors in primates, or general raptorial behaviors in birds. Predatory categories were sometimes considered separately because of distinct differences in foot use among raptorial birds during predatory

behavior, and corresponding morphological differences (Fowler et al., 2009). Where behavioral categories conflicted as in arboreal owls, predatory behavior took precedence.

Fowler et al. (2009) noted that owls are generally small prey specialists, and hypothesized that skeletal differences between owls and accipitrids corresponded to the relative frequency with which these taxa take larger prey, where large is defined as greater body size than can be completely enclosed in a flexed foot. However, some owls are known to take prey much larger than can be enclosed in a flexed foot (Marchesi et al., 2002; Lesmeister et al., 2010; Lloveras et al., 2011). Owl diets are often documented by skeletal remains in regurgitated pellets or nest observation, and there are known biases associated with these and other diet study methods, so the proportion of large prey items in owl diets may be higher than currently understood for some species (Real, 1996; Sanchez-Zapata and Calvo, 1998; Redpath et al., 2001; see Marchesi et al. 2002 for a review of these and other studies). Because structures must sometimes perform at the limits of their function to ensure survival, we expect that accipitrid and strigiform raptors should experience similar selective pressures (if only to varying degrees) relative to large prey acquisition despite the small prey specialization of most owl taxa and the tendency for accipitrids to take large prey more often. For this reason we test models where owls are included under the same and different behavioral optima from accipitrids.

All models are described in Tables 2-5. Behavioral assignments for each model are listed for all taxa in the appendix. Models were tested using the OUCH! package for OU models of selection in the statistical platform R. Because the continuous characters

are modeled separately there are no issues of co-linearity in the data. Model tests used the topologies recovered in the phylogenetic analyses, and each model was tested on one

Table 1 - Behavioral Regimes Used in Modeling Analyses and Associated Definitions

Behavior	Definition
Terrestrial	Does not often perform a vital function in raised, woody vegetation. Climbing ability limited or absent.
Arboreal	Regularly performs a vital function in raised woody vegetation.
Vertical Clinging	Regularly performs a vital function on sub-vertical surfaces (i.e. nesting, foraging, exudate feeding)
Predatory Accipitrid	Lengthy manipulation of live prey with the foot or feet; High proportion of "large" prey in the diet.
Predatory Falconid	Prey usually killed or immobilized prior to feeding; High proportion of "large" prey in the diet.
Predatory Strigiform	Lengthy manipulation of live prey with the foot or feet; Low proportion of "large" prey in the diet.

Table 2 - Models Tested for Primate Manual Intradigital Proportions

Model	Definition and Associated Hypothesis
PHB	A BM model, null hypothesis
PHOU1	An OU model with a single optimum H: The trait in question underwent the same directional or stabilizing selection pressure for all taxa.
PHOU2	An OU model with separate optima for terrestrial and arboreal primates H: mPE% and or mDE% is predictive of terrestriality vs. arboreality
PHOU3	An OU model with separate optima for terrestrial, arboreal, and vertical clinging/suspensory locomotion H: mDE% distinguishes between taxa that subject their phalanges to compressive stresses as in grasping behaviors, and taxa that subject their phalanges to tensile stresses as in vertical clinging.

Table 3 - Models Tested for Bird Pedal Intradigital Proportions

Model	Definition and Associated Hypothesis
BFB	A BM model, null hypothesis
BFOU1	An OU model with a single optimum
	H: The trait in question underwent the same directional or stabilizing selection pressure for all taxa.
BFOU2	An OU model with optima for terrestrial birds, and arboreal birds combined with predatory birds.
	H: Grasping behaviors such as perching exert similar selective pressures on phalangeal proportions to the behaviors associated with prey acquisition in raptorial birds.
BFOU3	OU model with separate optima for terrestrial birds, arboreal birds, and a combined optimum for vertical clinging birds and predatory birds
	H: Behaviors associated with prey acquisition in raptorial birds exert similar selection pressures (i.e. longitudinally oriented tensile loads) on phalangeal proportions to vertical clinging behaviors.
BFOU4	An OU model with separate optima for terrestrial, arboreal, vertical clinging, and predatory birds.
	H: Behaviors associated with prey acquisition in raptorial birds exert selection pressures that are manifest in differing proportional optima from vertical clinging taxa.
BFOU5	An OU model with separate optima for terrestrial taxa, arboreal taxa, and falconid raptors; and, a combined optimum or vertical clinging birds, accipitrid raptors, and strigiform raptors.
	H: Falconids are under differing selection pressure from all other birds
BFOU6	An OU model with an optimum for arboreal birds, a combined optimum for terrestrial birds and falconid raptors; and a combined optimum for vertical clinging birds, accipitrids, and Strigiformes.
	H: Falconids experience different selective pressures from other raptors, but are convergent on the same proportional optima as terrestrial taxa.

Table 4 - Models Tested for Mesozoic Theropod Manual Intradigital Proportions

Model	Definition and Associated Hypothesis
THB	A BM model, null hypothesis
THOU1	An OU model with a single optimum
	H: the trait in question underwent the same directional or stabilizing selection pressure for all taxa
THOU2	An OU model with separate optima for non-avian theropods and basal birds
	H: basal birds experienced selection pressures that manifest morphological differences from all other sampled theropods
THOU3	An OU model that includes microraptorines with basal birds in one optimum and all other non-avian theropods in a separate optimum.
	H: Microraptorines were experiencing selection for similar manual proportions to basal birds (i.e. elongation of the carpometacarpus)
THOU4	An OU model that hypothesizes differing optima for birds, small-bodied maniraptoran theropods, and the remaining theropods
	H: small bodied maniraptoran theropods experienced fundamentally different selection pressures from basal birds and larger theropods

thousand trees with random branch lengths to account for uncertainty in pace and path length of morphological change. Taxa for which the continuous characters were missing were pruned from the trees prior to model fitting. Internal branches were assigned behavioral regimes based on optimization of ancestral characters. Where optimizations were ambiguous, we used the DELTRAN algorithm, which maximizes trait convergence at the expense of reversals. In the mesozoic theropod data set, data for *Kol ghuva* were applied to the temporally and spatially contemporaneous parvicursorine alvarezsaur *Shuvuuia deserti*. *K. ghuva* was not used to estimate phylogeny, but it is assignable to the clade parvicursorinae, and its status as sister taxon to *Mononykus olecranus* in our pruned topologies makes its inclusion a negligible issue.

Table 5 - Models Tested For Mesozoic Theropod Pedal Intradigital Proportions

Model	Definition and Associated Hypothesis
TFB	A BM model, null hypothesis
TFOU1	An OU model with a single optimum
	H: the trait in question underwent the same directional or stabilizing selectio pressure for all taxa.
TFOU2	An OU model with separate optima for non-avian theropods and birds
	H: non-avian theropods experience selection pressures associated with cursoriality, while birds were free to evolve differing morphologies because of the disjunction of locomotor modules (Gatesy and Middleton, 1997).
TFOU3	An OU model with separate optima for birds, deinonychosaurian theropods, and all other non-avian theropods.
	H: Deinonychosaurian theropods experienced selection pressures on their pedal phalanges that manifest proportions similar to those in accipitrid and strigiform raptors (The RPR model) (Fowler et al., 2011).
TFOU4	An OU model with separate optima for birds, dromaeosaurid theropods, and the remaining non-avian theropods in the sample.
	H: The RPR model only applies to dromaeosaurids and not troodontids

Model Selection Criteria

Log-likelihoods for each model were calculated by OUCH! using a relative probability density function, so some log-likelihood values were negative (log of a relative probability between 0 and 1) and some were positive (log of a relative probability greater than 1). The Bayes Information Criterion (BIC) was calculated from each log-likelihood and the associated model parameters, and in all cases BIC values closer to negative infiniti are preferred. Standard deviations of log-likelihood and BIC values were

calculated to measure the relative dispersion of these model-fitting parameters in BM versus OU models. Because of the randomization of branch lengths for each model-fitting replicate, the recovered ranges of BIC values were often broad and overlapping, so each distribution was compared to those of competing models using Kolmogrov-Smirnov tests for differences in sampling distribution and two sided t-tests for differences in means. Models with the lowest or most-negative mean BIC were chosen as the best among considered models if they were also significantly different from the nearest model by KS-test and t-test.

It is important to note here how potential results will be interpreted. BM models can be interpreted as actual genetic drift, or stabilizing selection throughout the phylogeny in which natural phenotypic variation follows a normal distribution. Single optimum models are interpreted as uni-directional selection along all branches in the phylogeny. Multi-optimum models indicate directional selection at nodes where changes in assigned behavioral categories occur, because when a descendant branch or tip evolves towards a differing optimum from its sister taxon, there must be a directional shift in the values of the modeled trait.

RESULTS

Linear Measurements

The patterns we observed prior to model testing are similar to those that others have observed on smaller, more phylogenetically limited data sets. On average, terrestrial taxa tend to have shorter phalanges relative to their metacarpals, and arboreal taxa have the opposite pattern of lengthened phalanges relative to their metacarpals (Figures 1-3). Only two terrestrial mammals had mPE% shorter than 40%, the macropodiform marsupials *Sthenurus tindalei* and *Thylogale stigmatica*. The arboreal mammal with the highest mPE% was the long tailed porcupine *Trichys fasciculata* (53%). As others have noted, a pattern is present whereby taxa which exhibit habitual vertical clinging or suspensory postures for foraging or locomotion have proportionally higher mDE%, especially relative to mIE% (Hamrick et al., 1999; Frobisch and Reisz, 2009). This pattern is weak in primates (Figure 2), rodents, and marsupials, but there are strong outliers from the primary axis of variation in mammals such as dermopterans (colugos) and folivorans (sloths). This pattern was also strong in our reptile sample (Figure 3), where grasping arborealists (chameleons) had low mDE% and other arboreal reptiles had relatively higher mDE%. The feet of arboreal and terrestrial birds showed more overlap in ternary morphospace than the hands of arboreal and terrestrial tetrapods, but there is still a general trend of longer proximal elements (pPE%) in terrestrial taxa, and longer distal elements (pIE%, pDE%) in arboreal taxa (Figure 4). Accipitrid and strigiform

raptors (but not falconids) tend to have long penultimate phalanges (high pDE%, especially relative to pIE%), as do taxa that habitually forage or rest on vertical substrates such as woodpeckers, woodcreepers, and swifts.

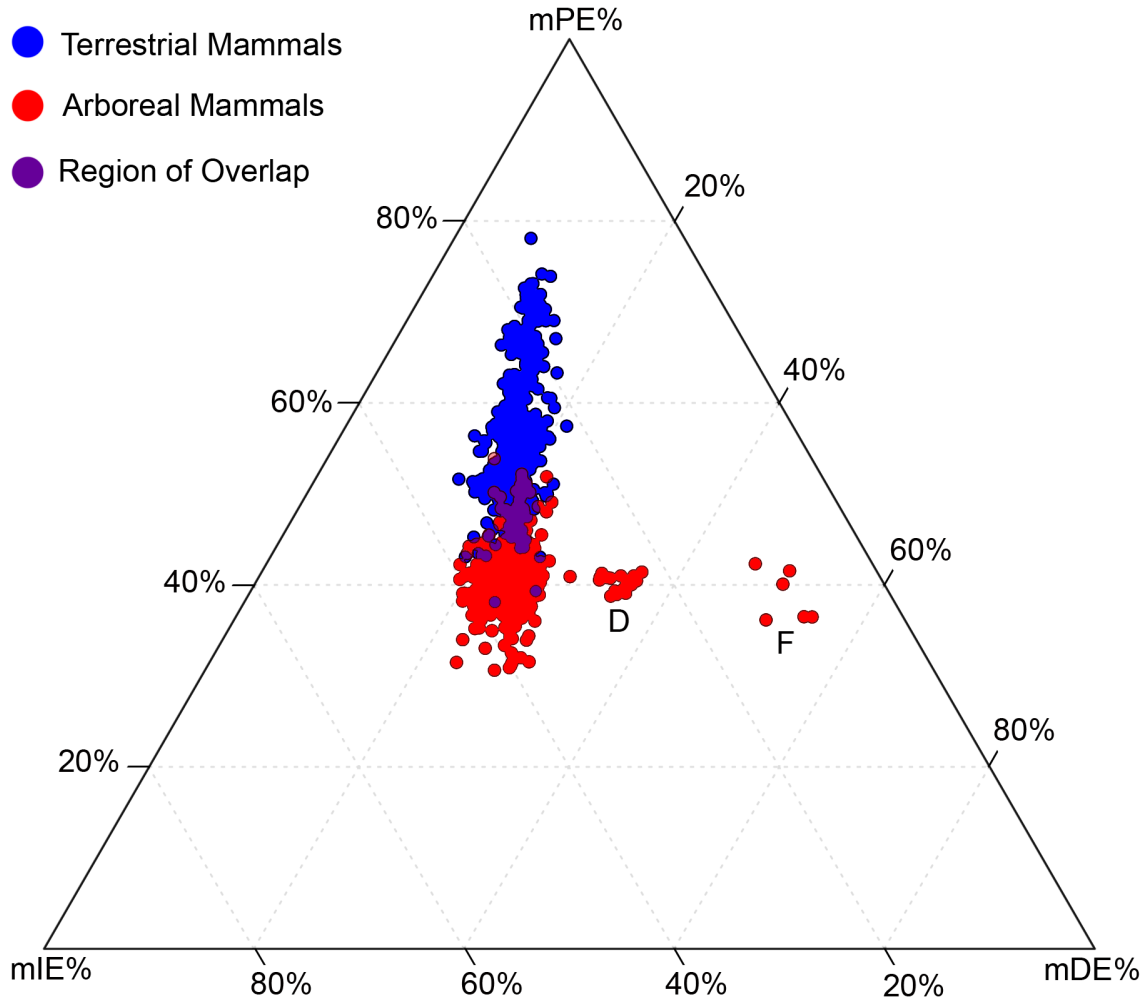

Figure 1. Distribution of Manual Phalangeal Proportions in Extant Mammals. Red circles represent arboreal mammals, blue circles represent terrestrial mammals, and purple circles represent co-occupation of morphospace by both terrestrial and arboreal mammals. D indicates a point cloud of dermopterans, F indicates a point cloud of folivorans. mPE%-the relative contribution of the metacarpal to the central digital ray, excluding the ungual; mIE%-the relative contribution of the most proximal manual phalanx to the central digital ray; mDE%-the relative contribution of the most distal non-ungual phalanx to the central digital ray.

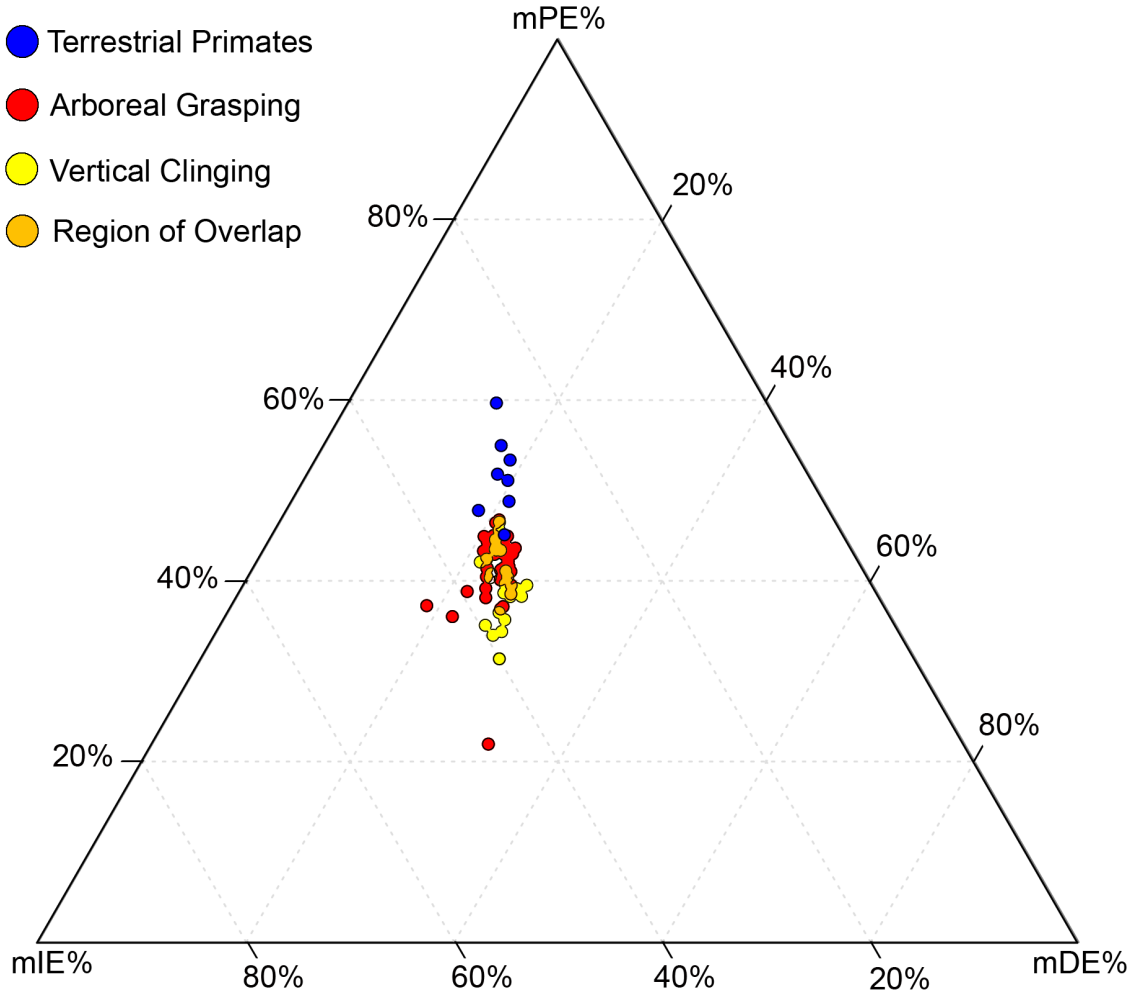

Figure 2. Distribution of Manual Phalangeal Proportions in Extant Primates. Red circles represent arboreal grasping primates, blue circles represent terrestrial primates, yellow circles represent vertical clinging primates, and orange regions represent co-occupation of morphospace by both arboreal grasping and vertical clinging primates. mPE%-the relative contribution of the metacarpal to the central digital ray, excluding the ungual; mIE%-the relative contribution of the most proximal manual phalanx to the central digital ray; mDE%-the relative contribution of the most distal non-ungual phalanx to the central digital ray.

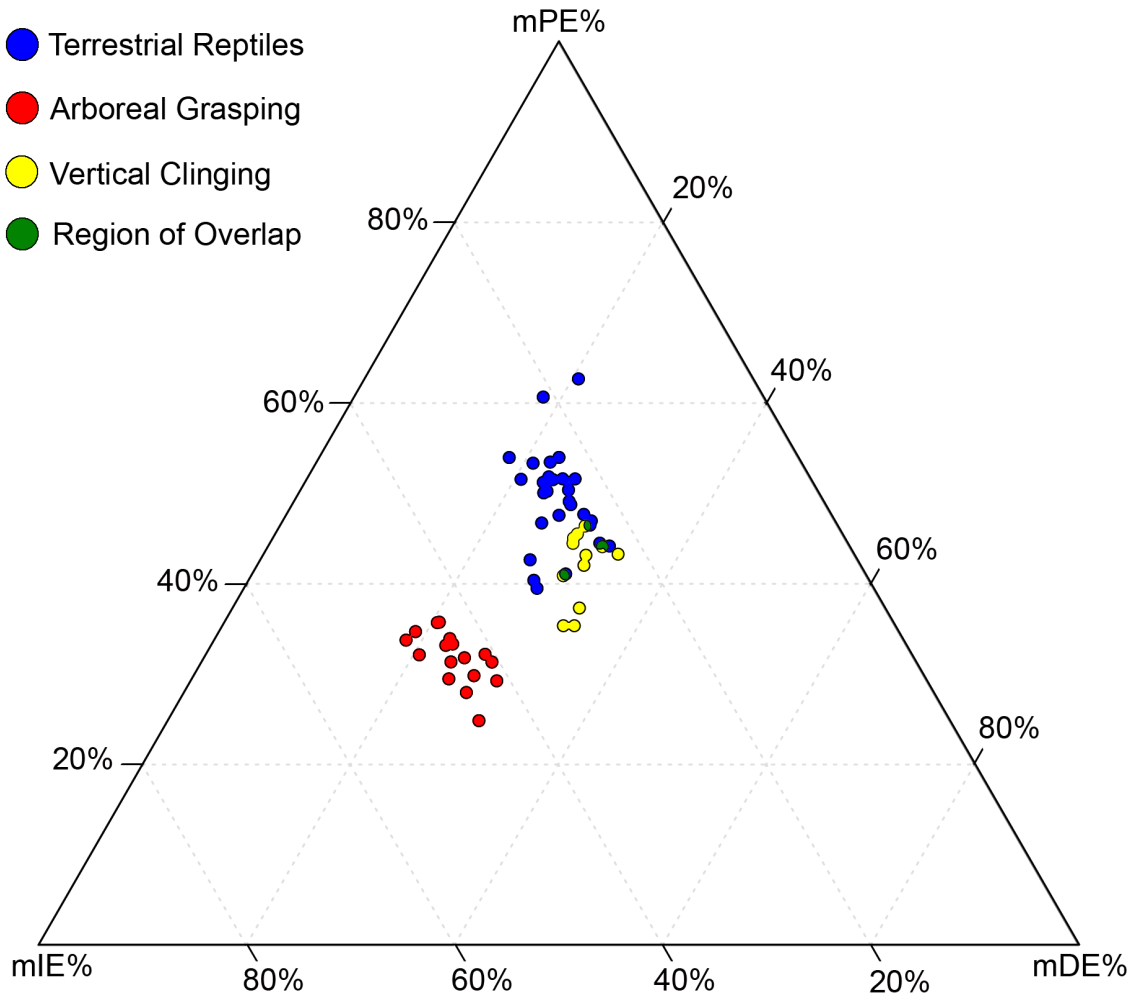

Figure 3. Distribution of Manual Phalangeal Proportions in Extant Reptiles. Blue circles represent terrestrial reptiles, red circles represent arboreal grasping reptiles (chameleonids), and yellow circles represent vertical clinging reptiles. mPE%-the relative contribution of the metacarpal to digital ray II excluding the ungual; mIE%-the relative contribution of the most proximal manual phalanx to digital ray II; mDE%-the relative contribution of the most distal non-ungual phalanx to digital ray II.

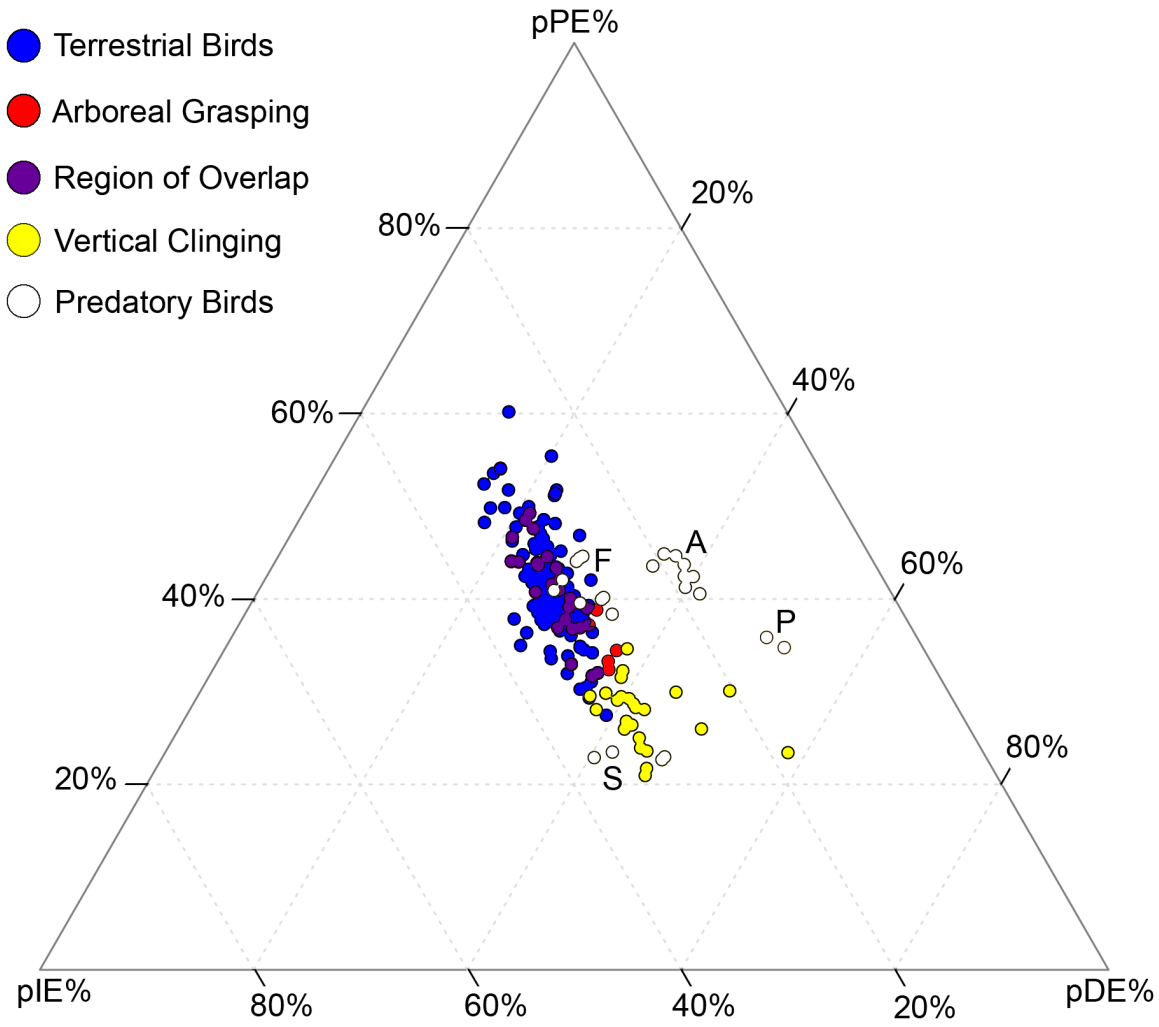

Figure 4. Distribution of Pedal Phalangeal Proportions in Extant Birds. Blue circles represent terrestrial birds; red circles represent arboreal grasping (or perching) birds; purple circles represent overlap between these two groups; yellow circles represent vertical clinging birds such as woodpeckers, woodcreepers, and swifts; white circles represent falconid, accipitrid, and strigiform raptors. F indicates a point cloud of falconids, A indicates a point cloud of accipitrids, S indicates a point cloud of Strigiformes, and P indicates two specimens of the accipitrid *Pandion*; pPE%-the relative contribution of phalanx III-1 to digital ray III, excluding the ungual; pIE%-the relative contribution of phalanx III-2 to the digital ray III, excluding the ungual; pDE%-the relative contribution of phalanx III-3 to digital ray III, excluding the ungual.

The hands of non-avian theropods share little morphospace with the hands of other tetrapods, although they do co-occupy space with dermopterans (Figure 5). The majority of taxa had mPE% at the upper range of extant arboreal tetrapods and the lower range of extant terrestrial tetrapods. Microraptorine dromaeosaurs had higher mPE% than any other paravians and the majority of sampled theropods. The only extant tetrapods with higher mDE% than non-avian theropods were folivorans. Four specimens of the oviraptorid "*Ingenia" yanshinii* were outliers from the primary cluster of non-avian theropods due to high mPE% (we add quotation marks around "*Ingenia*" in reference to the oviraptorid because the name is currently occupied by the nematode *Ingenia mirabilis).* The ceratosaurs *Limusaurus inextricabilis* and *Majungasaurus crenatissimus* were also outliers with high mPE% and the lowest mDE% among theropods.

The feet of non-avian theropods and mesozoic birds overlapped in morphospace with arboreal, terrestrial, and falconid extant birds, but not with accipitrid or strigiform raptors (Figure 6). Most non-avian theropods had higher pPE% than Mesozoic birds, but were otherwise similar in proportions. The scansoriopterygid *Epidendrosaurus ningchengensis* was a slight outlier from the primary cluster of non-avian theropods due to relatively low pPE% and correspondingly high pDE%.

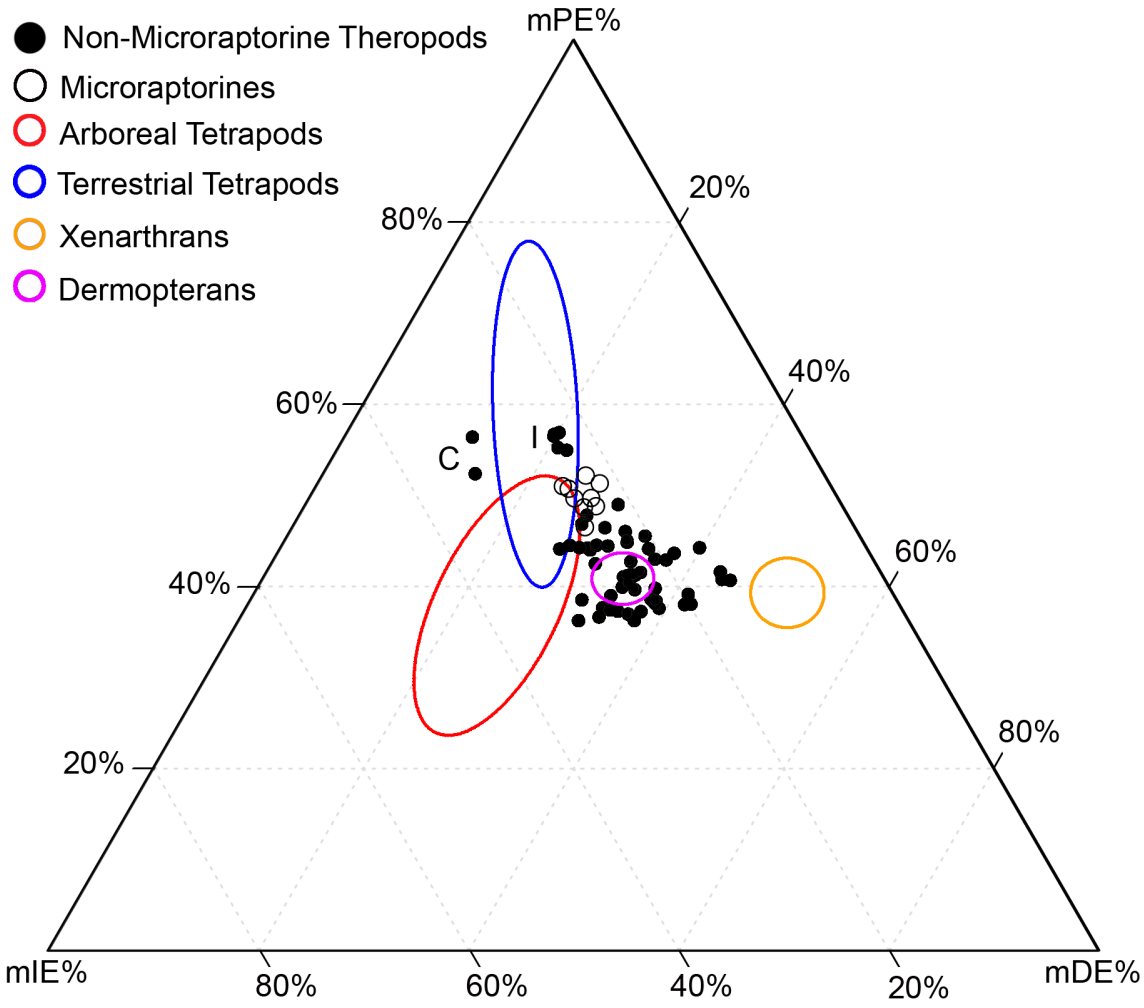

Figure 5. Distribution of Manual Phalangeal Proportions in Mesozoic Theropods. Colored ellipses represent morphospace occupied by extant taxa. Three basal birds are included, but do not diverge from the primary cluster. Note the amount of unshared morphospace between the hands of most sampled extant tetrapods and the theropods in this sample. Similarly to theropods, the dermopterans and folivorans each possess high mDE%. C - the two ceratosaurs in the sample. I - four specimens of the oviraptorid "*Ingenia*" clustered together. Microraptorines (open black circles) have higher mPE% than most other theropods. mPE%-the relative contribution of the metacarpal to the central digital ray, excluding the ungual; mIE%-the relative contribution of the most proximal manual phalanx to the central digital ray; mDE%-the relative contribution of the most distal non-ungual phalanx to the central digital ray.

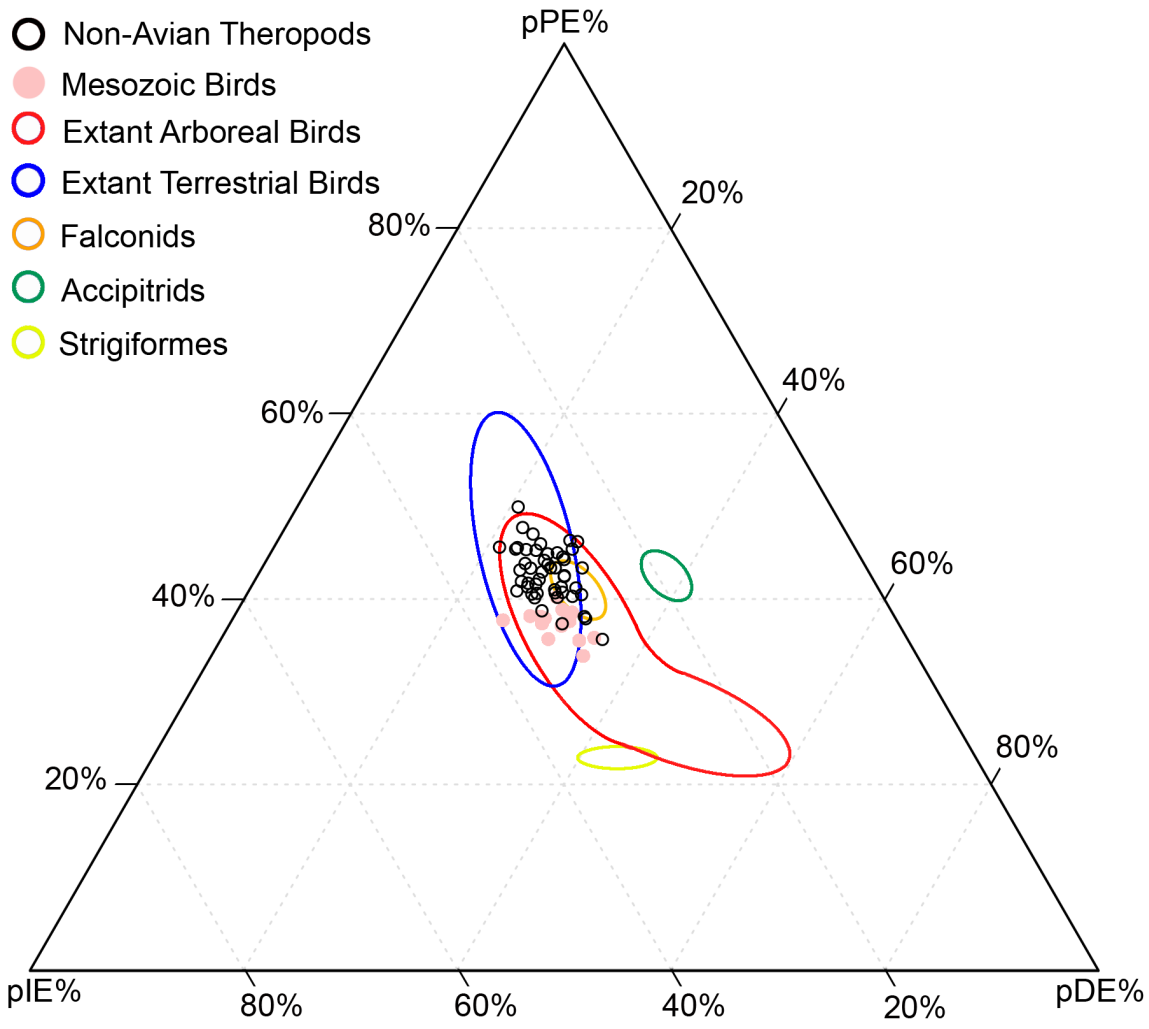

Figure 6. Distribution of Pedal Phalangeal Proportions in Mesozoic Theropods. Colored ellipses represent morphospace occupied by extant birds. Data from 5 basal bird species are included here. There is relatively low disparity among all mesozoic theropod feet, and they share morphospace with arboreal, terrestrial and falconid birds. Mesozoic theropods do not overlap in proportions with acippitrid or strigiform raptors. pPE%-the relative contribution of phalanx III-1 to digital ray III, excluding the ungual; pIE%-the relative contribution of phalanx III-2 to the digital ray III, excluding the ungual; pDE%-the relative contribution of phalanx III-3 to digital ray III, excluding the ungual.

Phylogenetic Analyses

The topologies recovered from the analyses of Neornithes and Primata were identical to those of Hackett et al. (2008) and Perleman et al. (2011), and bootstrap support was robust for the majority of clades in both cases, as in the original studies. The parsimony search for the mesozoic theropod matrix yielded 6048 most parsimonious trees 3306 steps, retention index of 0.614 and a consistency index of 0.198. The topology was uncontroversial and was similar in character to other iterations of the Theropod Working Group matrix (Turner et al., 2007; Makovicky et al., 2010). Trees are displayed in the appendix.

Evolution of Digital Ray Proportions

Model testing produced unanimous support for selection of manual and pedal proportions under 2, 3, and 4 regime models for the most proximal and most distal elements in each three- component system. The data suggest that intermediate elements follow brownian motion or single-optimum models of evolution, while the proximal and distal elements in each system evolve according to multiple directionally selective regimes. As expected from mathematical and evolutionary theory, brownian motion models had high standard deviations relative to OU models reflecting greater dispersion in model fitting parameters over a distribution of random branch-length trees. The best performing model for each trait according to BIC had a significantly different mean than the next best model by t-tests and differing distributions by Kolmogrov-Smirnov tests in

all cases. Summaries for model fitting on each manual and pedal element are discussed below.

The Hands of Primates

Model fitting results are summarized in Table 6, and density distributions of BIC are plotted for each model in Figure 7. *PHOU2*, a model with separate optima for arboreal and terrestrial taxa, performed best for the evolution of mPE%, followed closely by PHOU3, which assigned vertical clinging taxa to a separate optimum. Calculated mean optima for mPE% in *PHOU2* were 38.8% (sd=~2%) in arboreal taxa and 43.4% (sd=~1%) in terrestrial taxa. *PHB*, the brownian motion model, performed best by BIC for the evolution of mPE%. Calculated mean optima for mDE% in *PHOU3* were 23.9 %

Table 6. Model fitting summary for the hands of primates. Mll=mean log likelihood, SDll = standard deviation of the log likelihood distribution, mBIC=mean Bayes Information Criterion, SDbic=standard deviation of the BIC distribution

Model	**Trait**	**Mll**	**SDmll**	**Mean BIC**	**SDbic**
PHB	mPE%	127.8578	7.368371	-247.7564	14.03277
POU1	mPE%	132.6825	3.923984	-252.4126	7.847967
PHOU2	mPE%	143.8617	4.915888	**-266.1359**	9.831775
PHOU3	mPE%	143.7003	5.171525	-261.4956	10.34305
PHB	mIE%	-261.8028	5.681692	**532.2405**	11.36338
PHOU1	mIE%	-263.3274	4.735434	539.6072	9.470869
PHOU2	mIE%	-262.3702	4.914361	546.3278	9.828722
PHOU3	mIE%	-261.1546	5.076856	548.2142	10.15371
PHB	mDE%	157.1699	7.379708	-305.7048	14.75942
POU1	mDE%	162.104	4.081372	-311.2556	8.26174
PHOU2	mDE%	170.0113	4.540006	**-318.4351**	9.080013
PHOU3	mDE%	170.7885	4.638963	-315.6722	9.27793

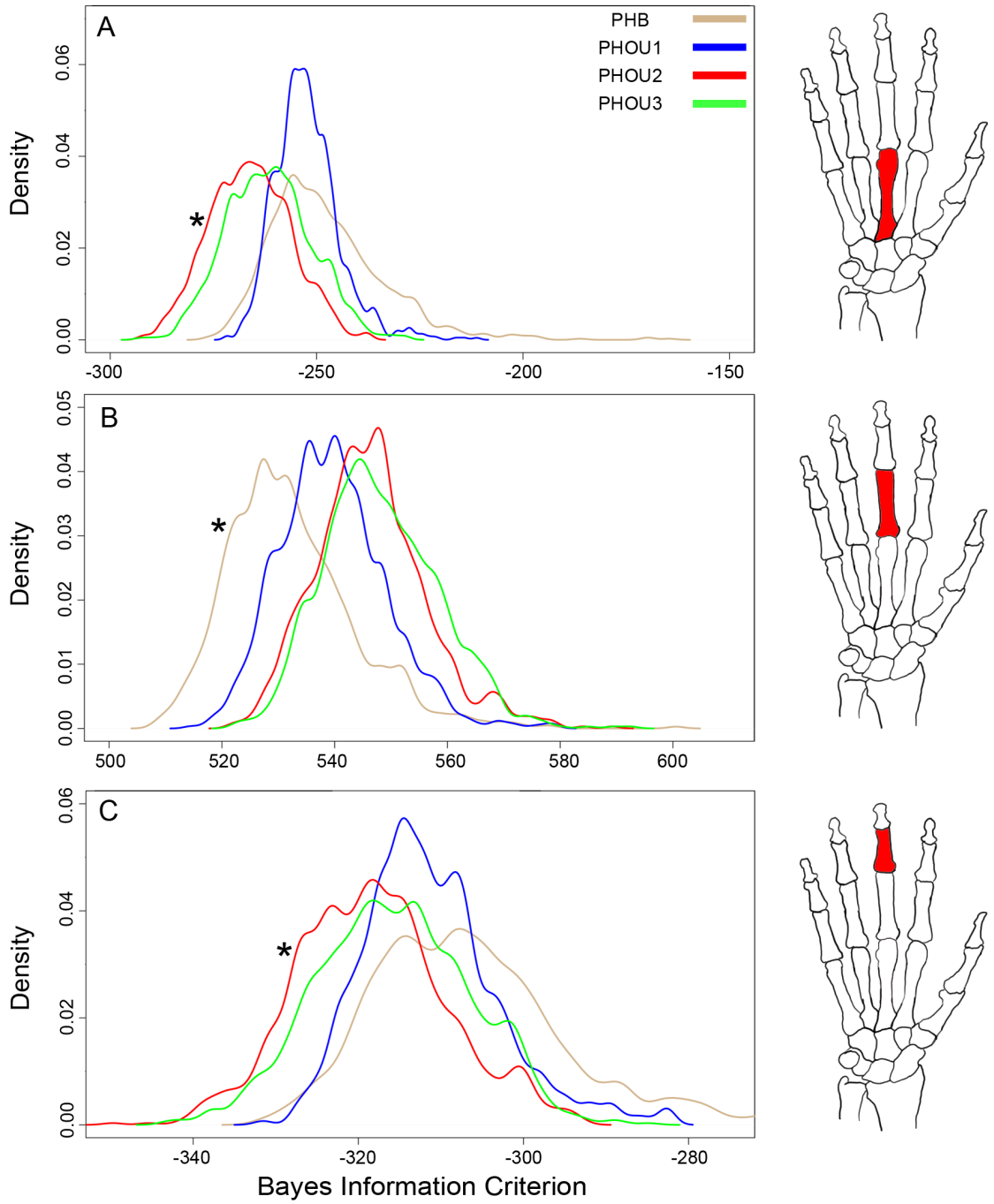

Figure 7. Density Distributions of BIC for Primate Hand Models (A) models fitting the evolution of mPE%, (B) models fitting the evolution of mIE%, and (C) models fitting the evolution of mDE%. Drawings at the right indicate the anatomical position of the modeled trait in red. Asterisks mark the density distribution curve for the optimum model for each trait.

(sd=1.6 %) in arboreal taxa and 27.1 % (sd=1.8 %) in vertical clinging taxa, so the differences in proportions between these two groups are apparent, but the pattern is not strong enough to improve upon a model driven by the arboreal/terrestrial dichotomy.

The Feet of Birds

Model fitting results are summarized in Table 7, and density distributions of BIC are plotted for each model in Figure 8. The model that combined vertical clinging taxa with accipitrid and strigiform raptors (*BFOU5*) performed best in modeling both pPE% motion model (THB). This is similar to the pattern seen previously in primate hands where for mPE% Brownian motion and the single optimum models also performed best. and pDE%. This model produced successively shorter mean optima for pPE% for terrestrial, falconid, arboreal and clinging birds (vertical clingers, accipitrids, and strigiformes). The opposite was true for pDE%, where *BFOU5* produced successively higher mean optima for terrestrial, falconid, arboreal, and clinging birds. For pIE%, a single optimum model (*BFOU1*) performed best by BIC, although *BFOU2* and *BFOU5* qualitatively appear to sample from the same density distribution as *BFOU1*, so this result may be related to sampling issues within the random branch lengths generated for the trees in these replicates.

The Hands of Mesozoic Theropods

Model fitting results are presented in Table 8, and density distributions of BIC are plotted for each model in Figure 9. Model testing chose *THOU3* (microraptorines

Table 7. Model fitting summary for the feet of birds. Mll=mean log likelihood, SDll = standard deviation of the log likelihood distribution, mBIC=mean Bayes Information Criterion, SDbic=standard deviation of the BIC distribution.

Model	Trait	Mll	SDmll	Mean BIC	SDbic
BFB	pPE%	174.866	11.0116	-340.0436	22.0232
BFOU1	pPE%	184.4611	5.291375	-354.3897	10.58275
BFOU2	pPE%	184.4802	5.059302	-354.4279	10.1186
BFOU3	pPE%	197.5738	4.105083	-366.0825	8.210167
BFOU4	pPE%	198.7275	3.979057	-363.5457	7.958114
BFOU5	pPE%	200.8211	3.797811	**-367.7329**	7.595622
BFOU6	pPE%	184.2115	5.514263	-353.8904	11.02853
BFB	pIE%	267.9094	9.711227	-526.1305	19.42245
BFOU1	pIE%	273.2191	4.990336	**-531.9057**	9.980672
BFOU2	pIE%	272.9191	5.078678	-531.3055	10.15735
BFOU3	pIE%	277.7465	4.635475	-526.4278	9.270951
BFOU4	pIE%	278.3409	4.884915	-522.7726	9.769829
BFOU5	pIE%	277.807	4.666883	-521.7047	9.333771
BFOU6	pIE%	273.0525	4.919974	-531.5725	9.839948
BFB	pDE%	178.3063	10.03661	-346.9242	20.07322
BFOU1	pDE%	183.7567	6.202653	-352.9808	12.4053
BFOU2	pDE%	183.8637	6.596087	-353.1948	13.19217
BFOU3	pDE%	204.1561	5.210055	-379.2471	10.42011
BFOU4	pDE%	205.1969	5.277942	-376.4844	10.55589
BFOU5	pDE%	210.3638	5.514623	**-386.8184**	11.02925
BFOU6	pDE%	184.1439	5.963684	-353.7553	11.92737

convergent with basal birds) by BIC in both mPE% and mDE%. This is reflective of the elongation of metacarpals and corresponding reduction of the manual penultimate phalanx. The single optimum model performed best for mPE% followed by the brownian motion model (*THB*). This is similar to the pattern seen previously in primate hands where for mPE%, brownian motion and the single optimum models also performed best.

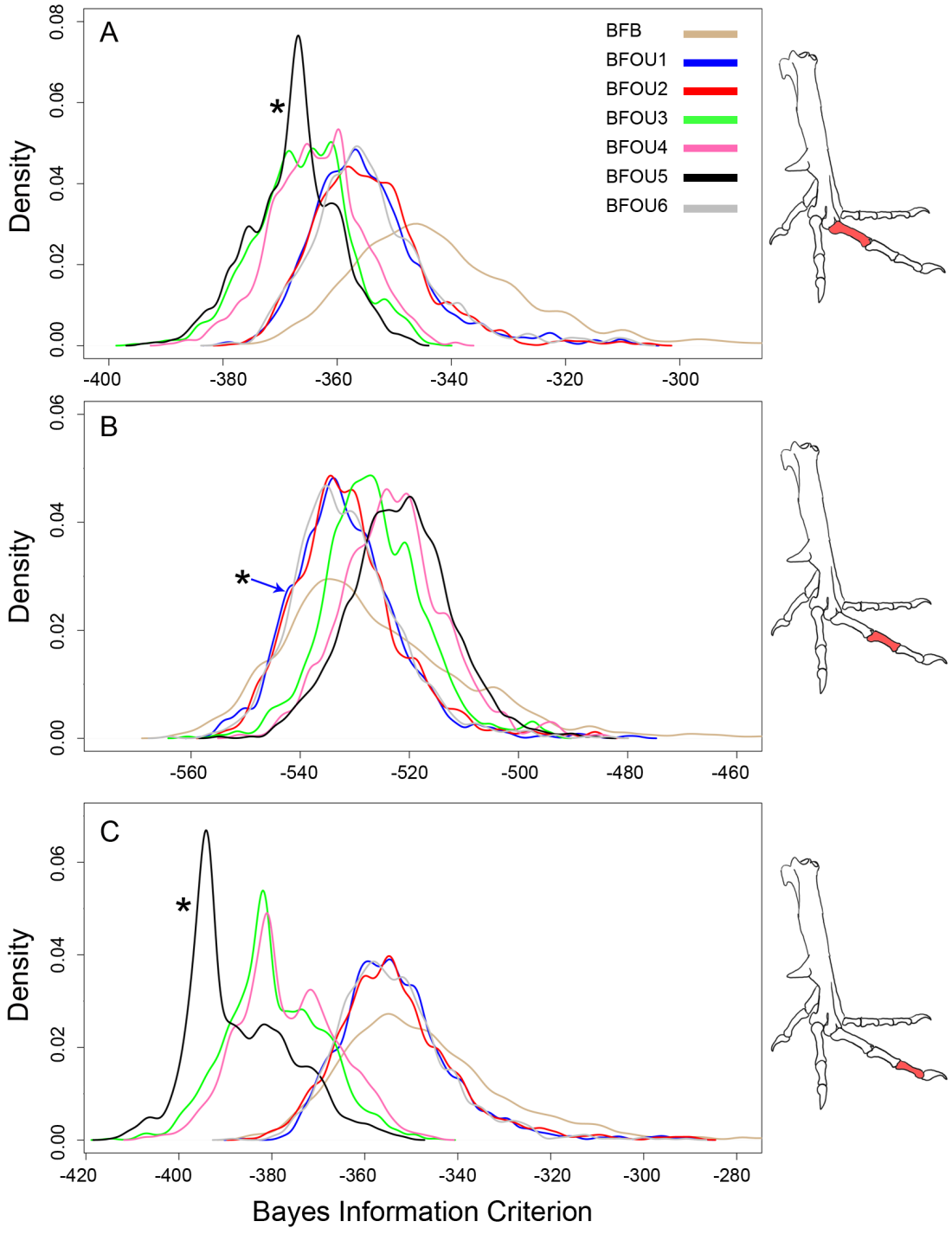

Figure 8. Density Distributions of BIC for Bird Foot Models. (A) models fitting the evolution of pPE%, (B) models fitting the evolution of pIE%, and (C) models fitting the evolution of pDE%. Drawings at the right indicate the anatomical position of the modeled trait in red. Asterisks mark the density distribution curve for the optimum model for each trait.

Table 8 - Model Fitting Summary for the Hands of Mesozoic Theropods. Mll=mean log likelihood, SDll = standard deviation of the log likelihood distribution, mBIC=mean Bayes Information Criterion, SDbic=standard deviation of the BIC distribution

Model	Trait	Mll	SDll	mBIC	SDbic
THB	mPE%	55.93349	3.867984	-104.3916	7.735968
THOU1	mPE%	62.91373	0.886695	-114.6144	1.773392
THOU2	mPE%	63.49483	1.156739	-108.3013	2.313477
THOU3	mPE%	68.58539	1.465635	**-118.4824**	2.931270
THOU4	mPE%	63.97728	1.228134	-105.5285	2.456268
THB	mIE%	79.18965	4.247451	151.4809	10.85669
THOU1	mIE%	82.64778	2.137788	**-154.0825**	4.275577
THOU2	mIE%	83.63895	2.261181	-148.5896	4.522365
THOU3	mIE%	83.97307	2.403161	-149.2578	4.806322
THOU4	mIE%	84.44142	2.32839	146.4568	4.65678
THB	mDE%	50.906	4.216576	-94.63575	7.898287
THOU1	mDE%	56.02864	1.284763	-100.8443	2.569527
THOU2	mDE%	56.85966	1.420727	-96.28265	11.80382
THOU3	mDE%	60.92192	2.01965	**-103.1555**	4.039301
THOU4	mDE%	57.06351	1.547164	-91.70099	3.094329

<u>The Feet of Mesozoic Theropods</u>

Model fitting results are presented in Table 9, and density distributions of BIC are plotted for each model in Figure 10. A relatively simple model for theropod feet (*TFOU2*) performed best in which the five basal birds in the dataset were assigned to a separate regime from all non-avian theropods due to their relatively low pPE%. Whereas modern birds with predatory foot use were easily recognizable with these methods based on the relative success of *BFOU5* for pPE% and pDE%, a shift in selection pressure was

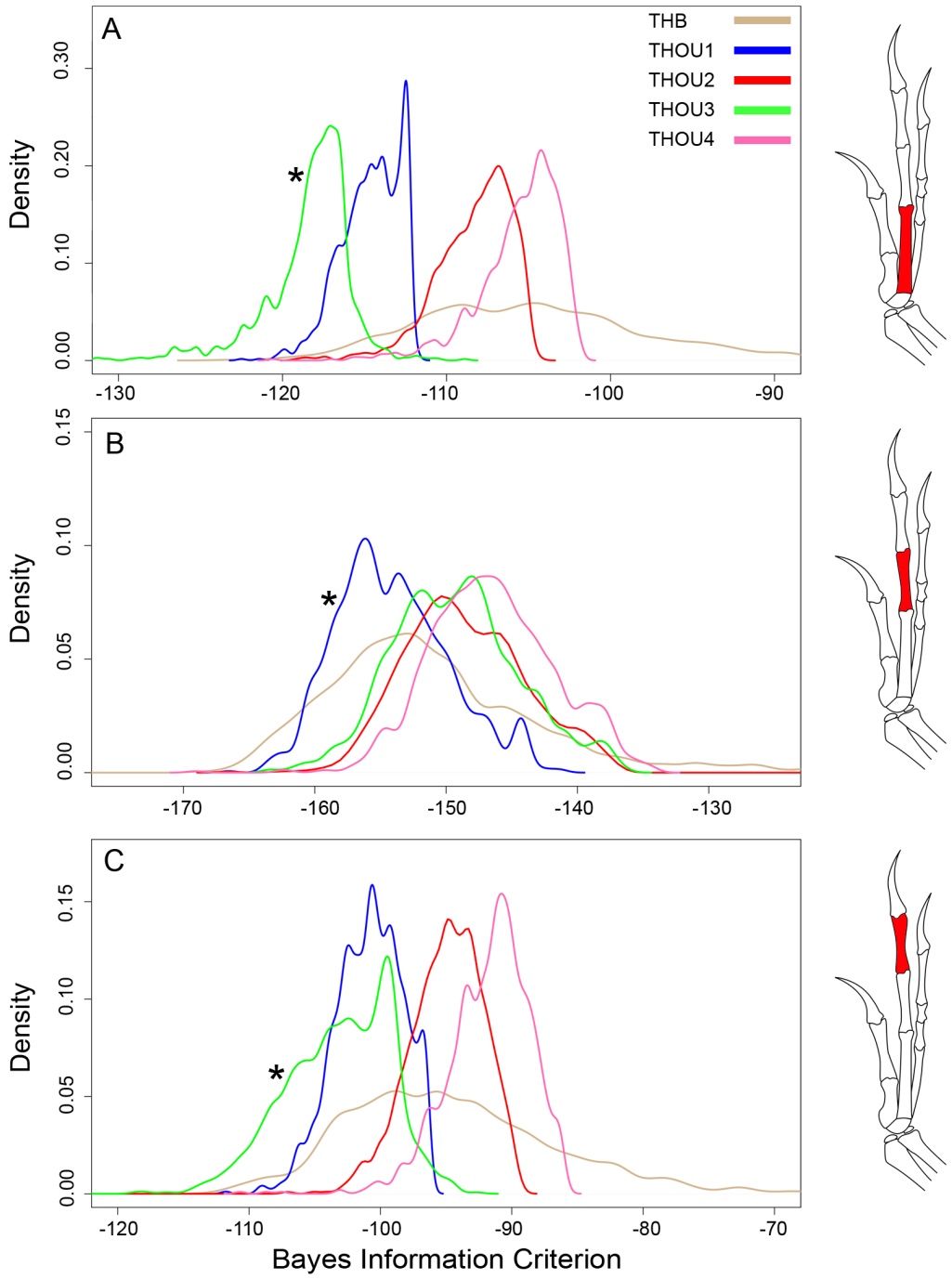

Figure 9. Density Distributions of BIC for Mesozoic Theropod Hand Models. (A) models fitting the evolution of mPE%, (B) models fitting the evolution of mIE%, and (C) models fitting the evolution of mDE%. Drawings at the right indicate the anatomical position of the modeled trait in red. Asterisks mark the density distribution curve for the optimum model for each trait.

Table 9 - Model Fitting Summary for the Feet of Mesozoic Theropods. Mll=mean log likelihood, SDll = standard deviation of the log likelihood distribution, mBIC=mean Bayes Information Criterion, SDbic=standard deviation of the BIC distribution

Model	Trait	Mll	SDmll	Mean BIC	SDbic
TFB	pPE%	76.89912	3.419356	-146.2978	6.644049
TFOU1	pPE%	84.06476	0.7340836	-156.9888	1.468165
TFOU2	pPE%	88.91331	1.14505	-159.2588	2.290101
TFOU3	pPE%	89.62443	1.158559	-156.9674	2.317117
TFOU4	pPE%	89.65332	1.286104	-153.3116	2.572208
TFB	pIE%	96.01561	3.593864	-184.5877	6.971186
TFOU1	pIE%	106.2042	0.3242936	-201.2475	0.5688743
TFOU2	pIE%	107.1651	0.9322663	-195.787	1.99053
TFOU3	pIE%	109.406	1.021977	-196.4567	2.027152
TFOU4	pIE%	109.4235	1.106697	-192.796	2.056434
TFB	pDE%	70.34721	5.21137	-134.0353	9.366821
TFOU1	pDE%	81.61531	0.3852739	-152.0899	0.7705421
TFOU2	pDE%	86.03315	1.041827	-153.4984	2.083654
TFOU3	pDE%	86.15643	1.261876	-150.0314	2.523751
TFOU4	pDE%	86.20619	1.18991	-146.4174	2.37982

not observed for Deinonychosauria. Deinonychosaurians (*TFOU3*) and dromaeosaurids but not troodontids (*TFOU4*) were assigned separate selective regimes in these models, but while they outperformed BM (*TFB*), *TFOU3* and *TFOU4* were significantly worse than *TFOU2*.

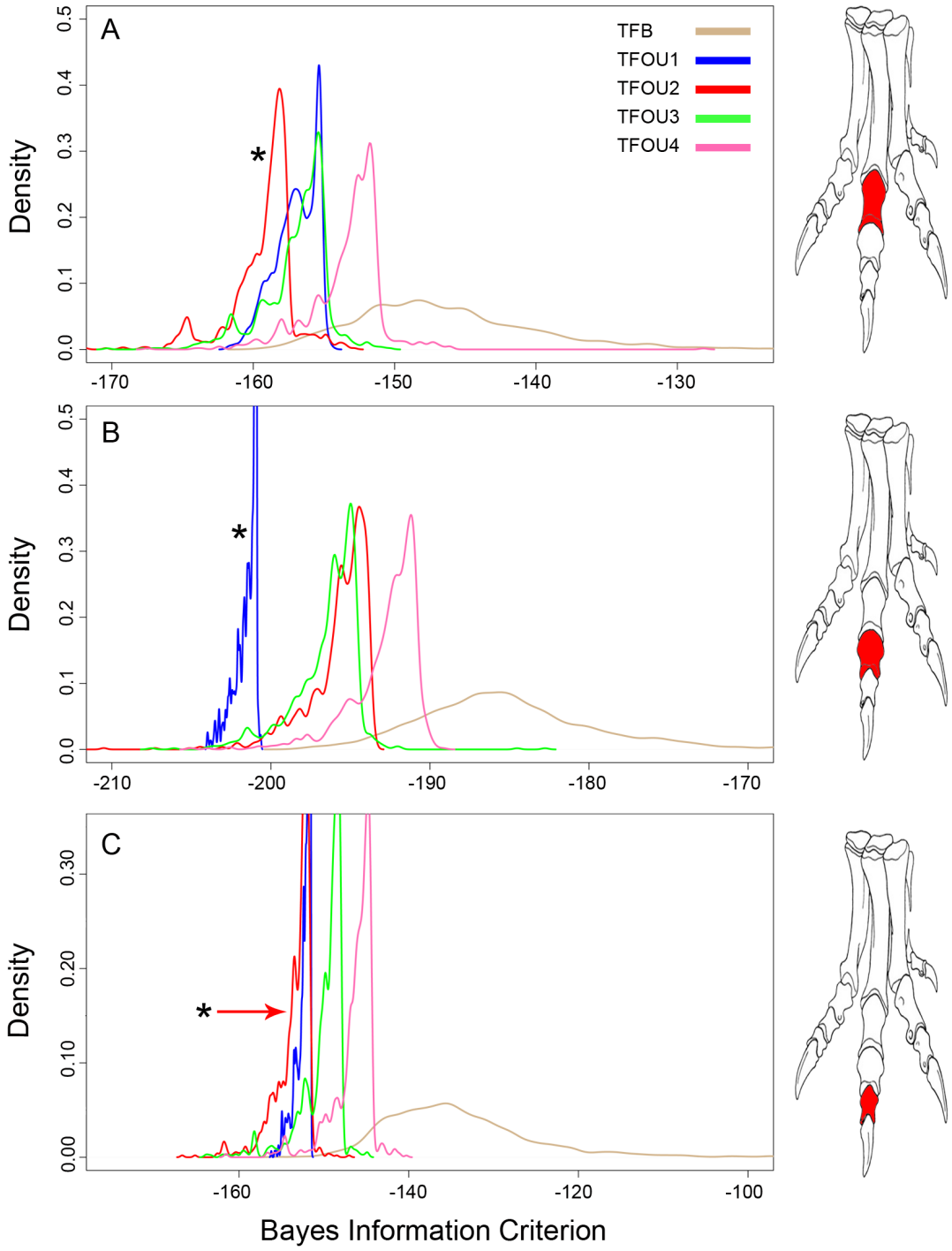

Figure 10. Density Distributions of BIC for Theropod Foot Models. (A) models fitting the evolution of pPE%, (B) models fitting the evolution of pIE%, and (C) models fitting the evolution of pDE%. Drawings at the right indicate the anatomical position of the modeled trait in red. Asterisks mark the density distribution curve for the optimum model for each trait.

DISCUSSION

The results of model testing conformed well with observed qualitative associations of traits and behaviors for birds and primates. Nearly every OU model tested explained the data better than brownian motion. These results combined with the original misgivings of Felsenstein (1985) regarding BM applied using phylogenetically independent contrasts suggest a shift toward using selective models such as those implemented here are necessary for future comparative phylogenetic studies. OU models and methods could be tested on a given data set, an optimum model would be selected as in this study, and then that model would be applied in an analysis using phylogenetic comparative methods rather than assuming a brownian motion model of character evolution.

In the general case, reconstruction of ancestral trait use patterns is necessary to improve the realism of proposed models in this framework, but beyond the simple optimization at ancestral nodes there is little room for realistic advancement of methods in this realm because phylogenetic studies can not identify ancestors. Assigning a single optimum to all internal branches of a phylogeny is one option that reduces the number of estimated parameters and removes error associated with those estimations; but, only at the cost of applying a false assumption to the model. Uncertainty in character optimization is exacerbated in cases where taxon sampling is not robust, such as in the pruned mesozoic theropod phylogeny used here. For this reason we are cautious about

making functional interpretations for theropods based on our modeling observations, however there are several points to discuss.

Based on observed qualitative patterns and the results of evolutionary modeling, arboreal and terrestrial lineages evolve in opposite directions with respect to the most proximal elements in the systems examined here (i.e. mPE% in the hands of primates and pPE% in the feet of birds). Terrestrial organisms characteristically have relatively long proximal elements in the three-component systems we examined, while arboreal taxa generally evolve longer distal elements. The preference for multi-optimum models rather than brownian motion or single optimum models indicates the persistence of directional selection in lineages through time for these characters.

Model selection criteria showed that the intermediate elements of the systems we investigated evolved by brownian motion, or single optimum models for all characters. We interpret this as either the determinance of relative intermediate element length by stochastic changes in the other two elements, or as stabilizing selection for the maintenance of proportionality.

The performance of a multi-optimum model for the evolution of proximal and distal elements in theropod hands suggests that the historical attribution of grasping functionality is an oversimplification and is probably erroneous according to behavioral definitions for grasping and clinging. The similarity in proportions of some theropod hands (notably non-microraptorine paravians) with those of animals that habitually cling to large diameter substrates may be indicative of similar mechanical loading and/or

functionality. These large diameter substrates could include prey items or perhaps even tree trunks for long-armed, smaller-bodied taxa.

Our study produced an interesting result with respect to the climbing ability of theropods in that the optimum model for the hands of mesozoic theropods (*THOU3*) suggests microraptorine dromaeosaurs as the least likely theropods in the data set to have used their hands to climb trees. The model hypothesizes that microraptorines and mesozoic birds underwent selection for longer metacarpals relative to their phalanges, which is similar to the process modeled for terrestrial primates in this study, and is congruent with a shift away from a grasping or clinging morphology based on our qualitative observations in other terrestrial tetrapods. The similarity with terrestrial primates in selection for relative elongation of the carpometacarpus is unlikely to be reflective of similar functionality, as terrestrial primates use their hands in quadrupedal locomotion, and microraptorines and Mesozoic birds clearly did not. What it does indicate is a similar movement away from the typically paravian morphology in microraptorines and away from the typical morphology found in arboreal primates that may be related to a reduction in ability to manipulate objects, whether by grasping or clinging behaviors. It has been previously suggested that shortened phalanges (and thus relatively longer metacarpals) function in reducing bending moments associated with ground reaction forces in quadrupedal terrestrial taxa (Jolly, 1967; Patel et al., 2009). This is congruent with our results for primates but does not explain the modeled selection for the increase in metacarpal length for microraptorine dromaeosaurids and basal birds, or

the elongate metacarpals of "Ingenia", *Limusaurus*, and *Majungasurus*. Potential explanations for the convergently high mPE% in birds and microraptorines are the need for additional surface area for the attachment of primary remiges on the carpometacarpus relative to the phalanges, or perhaps the restriction of flexibility to the more distal portions of the wing creating a more rigid structure for the resistance of forces associated with lift or drag in flapping flight, gliding, stability flapping (Fowler et al., 2009), or flapping display behaviors. Most flighted birds possess a phalangeal portion of the hand shorter than the carpometacarpus, although Mayr (2005) found a longer phalangeal portion of the manus as a synapomorphy of Cypselomopha (Caprimulgiformes, Apodiformes, and Trochiliformes). We have not collected data to test this hypothesis and we know of no study that examined the intradigital proportions of the avian hand comprehensively, but if the elongation of the carpometacarpus relative to the phalanges is a feature associated with flight performance in typical avian flight or gliding, it may indicate that microraptorines evolved one or both of these capabilities convergently with birds.

Three other non-avian theropods in the sample had high mPE% ("Ingenia, *Limusaurus*, and *Majungasaurus*), but were not included in the same behavioral optimum with microraptorines and birds in *THOU3* or any other model. No known fossils of "*Ingenia*" have associated feathers or their impressions, as this type of preservation is not common in the Nemegt formation of Mongolia where they are found. Other oviraptorids are known to possess feathers (Ji and Ji, 1997; Ji et al., 1998; Zhou and Wang, 2000; He

et al. 2008) so it is likely that "*Ingenia*" did as well, but we were unwilling to speculate if the length of these potential feathers were similar to those seen in microraptorines and birds. These fact combined with their relatively large body size and reduced forelimbs compared to microraptorines and basal birds precluded their assignment to the same behavioral optimum as these taxa in *THOU3* despite high mPE%. *Limusaurus* and *Majungasaurus* both possess extremely reduced forelimbs and hands, so their relatively high mPE% is presumably associated with this reduction, or they were at least dissimilar in forelimb function to microraptorines and birds.

In general, the hands of most non-avian and non-microraptorine theropods experienced similar selection in these models to the feet of raptorial and vertical-clinging birds. Although these results fail to reject arboreality in mesozoic theropods, we should stress that these models can only hypothesize similar selective pressures, and not similar functions. However, these results do support the hypothesis that elongation of the penultimate phalanges is related to longitudinally oriented tensile stresses in these elements, and not perpendicularly oriented compressive stresses that would be habitually experienced if grasping were the dominant function in the hand. Predatory use of the hand in clawed adhesion to prey items larger than the grasping radius, and/or adhering to subvertical vegetation seem more likely. Of course, this does not rule out alternate explanations for elongate penultimate phalanges such as simply adjusting the position of the unguals beyond primary feathers projecting from the carpometacarpus.

A simplistic multi-optimum model (*TFOU2*) for the evolution of Mesozoic theropod feet is difficult to interpret, but we can offer a few potential explanations. The behavioral hypotheses of this model indicated that feet experienced different selection pressures in non-avian and avian taxa, and while this may be generally true it is likely that this is an underestimation of the complexity of evolution and functional diversity for mesozoic theropod feet. Models that hypothesized separate and perhaps predatory functional regimes in the feet of deinonychosaurians performed better than *TFB* (a BM model) but worse than *TFOU2*. While a shift in selection pressure may have only occurred near the origin of flight, it is more likely that the characters studied, the taxa sampled, or the hypothesized models failed to adequately characterize variation in habitual foot use for non-avian theropods or that there is a sampling gap that covers the regime change hypothesized by the model (*TFOU2*). This will be a general problem any time this type of analysis is applied to fossil taxa, especially if the characters under study require complex information from multiple elements. Nevertheless, the "Raptor Prey Restraint" model for pedal function in deinonychosaurians is not supported by our data.

The pedal phalangeal proportions of microraptorines were consistent with those of most other non-avian theropods, which co-occupied morphospace in an overlapping region where both arboreal and terrestrial birds plotted. It is apparent from these modeling results that the hands of microraptorines evolved in a manner similar to birds; and, that the feet of microraptorines evolved similarly to the feet of other mesozoic theropods without experiencing selection for reduction in pPE% as Mesozoic birds in the

sample did (*TFOU2*). Thus, there is no evidence to support the specialization of microraptorines for an arboreal lifestyle, potentially contradicting previous assertions that microraptorines were arboreal (Xu et al., 2000; Xu et al. 2003; Zhou et al., 2004; Burnham, 2007).

Epidendrosaurus was a slight outlier in pedal phalangeal proportions from other non-avian theropods in our sample with the lowest pPE% for non-avian theropods (35.7%), was among the theropods with the lowest mPE% (38.7%), and had a high mDE% (38.4%) among maniraptorans. Like microraptorines, *Epidendrosaurus* has been explicitly hypothesized to be arboreal (Zhang et al., 2002; Zhou et al., 2004), and low MPE%, high mDE%, and low pPE% are all consistent with vertical clinging and/or arboreal habits according to our qualitative observations in the hands of extant tetrapods and our modeled results in the feet of birds. However, this taxon is known from only two immature and extremely small specimens and its status as an outlier in pedal proportions may be related to scaling effects related to small body-size or allometric changes in pedal phalangeal proportions during ontogeny (although we did not recognize any other indicators of size or ontogenetic scaling effects in our data set). Regardless, the model hypothesizing small-bodied maniraptorans (including *Epidendrosaurus*) as belonging to a different selective regime from microraptorines, birds, and other non-avian theropods (*THOU4*) was the worst among five models tested for theropod hands for mIE% and mDE%, and the second worst (to THB) for mPE%. Arboreality in *Epidendrosaurus*

remains an interesting hypothesis given the peculiar manual and pedal proportions in this taxon, but it is unsupported by this analysis.

Further tests of additional traits including more complex assignments of hypothesized behavioral regimes have the potential to improve our understanding of hand and foot use in theropods. We urge future researchers to test OU models on their data prior to using phylogenetically independent contrasts, square change parsimony, and other phylogenetic comparitive methods that assume character evolution by brownian motion. Additional verification of the efficacy of these models and improvement upon their methods should be done on laboratory organisms living under environmentally controlled selective regimes. (e.g. *D. melanogaster, C. elegans*)

REFERENCES CITED

Beaulieu, J.M., S.A. Smith, and I.J. Leitch. (2010). "On the tempo of genome size evolution in angiosperms." *Journal of Botany,* vol. **2010,** Article ID 989152.

Bloch, J.I., and D.M. Boyer. (2002) "Grasping primate origin". *Science* **298**(5598): 1606-1610.

Boyer, D. M., & Bloch, J. I. (2008). "Evaluating the mitten-gliding hypothesis for paromomyidae and micromomyidae (Mammalia , " Plesiadapiformes ") using comparative functional morphology of new Paleogene skeletons. In E. J. Sargis & M. Dagosto (Eds.), Mammalian Evolutionary Morphology: A Tribute to Frederick S. Szalay, pp. 233-284. Springer, Dordrecht, The Netherlands.

Burnham, D. A. (2007). "Archaeopteryx – a re-evaluation suggesting an arboreal habitat and an intermediate stage in trees down origin of flight." *Neues Jahrbuch für Geologie und Paläontologie Abhandlungen*, **245**(1), 33-44.

Butler, M. and A. King. (2004). "Phylogenetic comparative analysis: a modeling approach for adaptive evolution." *American Naturalist* **164**:683-695.

Carvalho P., J. Diniz-Filho, and L. Bini (2006) "Factors influencing changes in trait correlations across species after using phylogenetic independent contrasts." *Evolutionary Ecology* **20**:591-602.

Cartmill, M. (1985). "Climbing". In M. Hildebrand, K.F. Liem, D.M. Bramble, and D.B. Wake (Eds.). Functional Vertebrate Morphology. Belknap Press. Harvard.

Cartmill, M. (1992). "New views on primate origins." *Evolutionary Anthropology* **1**: 105-111.

Chatterjee, S., and R.J. Templin (2004). "Feathered coelurosaurs from China: new light on the arboreal origin of avian flight." In P. J. Currie, M. A. Koppelhaus, M. A. Shugar, & W. J. L (Eds.), Feathered Dragons Studies on the Transition from Dinosaurs to Birds. pp. 251-281. Indiana University Press. Bloomington, Indiana.

Choiniere, J. N., J.M. Clark, C.A. Forster, and X. Xu. (2010). "A basal coelurosaur (Dinosauria: Theropoda) from the Late Jurassic (Oxfordian) of the Shishugou Formation in Wucaiwan, People's Republic of China." J*ournal of Vertebrate Paleontology*, **30**(6), 1773-1796.

Colbert, E. H. (1989). The Triassic dinosaur *Coelophysis*. *Bulletin of the Museum of Northern Arizona*, **53**:1-61.

Collar, D.C., B.C. O'Meara, P.C. Wainwright, and T.J. Near. (2009). "Piscivory limits diversification of feeding morphology in centrarchid fishes". *Evolution* **63**:1557-1573.

Elphick, C., J.B. Dunning, and D.A. Sibley (eds.) (2001). The Sibley Guide to Bird Life and Behavior. Chanticleer Press, New York.

Felsenstein, J. (1985). "Phylogenies and the comparative method." *American Naturalist* **125**:1-15.

Fleagle, J.G. (1999). Primate Adaptations and Evolution, second ed. Academic Press, New York.

Fowler, D. W., E.A. Freedman, and J.B. Scannella (2009). "Predatory functional morphology in raptors: interdigital variation in talon size is related to prey restraint and immobilisation technique." *PLoS One*, **4**(11), e7999.

Fowler, D.W., E.A. Freedman, J.B. Scanella, and R.E. Kambic (2011) "The predatory ecology of Deinonychus and the origin of flapping in birds." *PLoS One* **6**(12): e28964.

Frobisch, J. and R. Reisz. (2009). "The Late Permian herbivore *Suminia* and the early evolution of arboreality in terrestrial vertebrate ecosystems." *Proceedings of the Royal Society B*. **276**:3611-3618

Grafen, A. (1989). "The phylogenetic regression." *Philosophical Transactions of the Royal Society of London B.* **326**:119–157.

Gatesy, S.M. and K.M. Middleton. (1997). "Bipedalism, flight, and the evolution of theropod locomotor diversity." *Journal of Vertebrate Paleontology* **17**:308-29.

Gauthier, J. A., and K. Padian. (1985). "Phylogenetic, functional, and aerodynamic analyses of the origin of birds and their flight." In M. K. Hecht, et al. (eds.), The Beginnings of Birds, pp. 185–197. Freundo des JuraMuseums, Eichstatt, Germany.

Gilmore, C. W. (1920). "Osteology of the carnivorous dinosauria in the United States National Museum, with special reference to the genera *Antrodemus* (*Allosaurus*) and *Ceratosaurus*." *Bulletin of the United States National Museum*, **110**:1-159.

Gishlick, A. D. (2001). "The functional morphology of the manus and forelimb of *Deinonychus antirrhopus* and its importance for the origin of avian flight." In J. A. Gauthier (ed.), Perspectives on the origin and evolution of birds. Yale University Press, New Haven.

Goloboff, P. A., S. Farris, and K.C. Nixon. (2003). "T.N.T.: Tree Analysis Using New Technology. 1.1". Tucumán, Argentina: The authors.

Hackett, S. J., R.T. Kimball, S. Reddy, R.C.K. Bowie, E.L. Braun, M.J. Braun, J.L. Chojnowski et al. (2008). "A phylogenomic study of birds reveals their evolutionary history." *Science*. **320**(5884): 1763-1768.

Hamrick, M. W., B.A. Rosenman, and J.A. Brush (1999). "Phalangeal morphology of the Paromomyidae (?Primates, Plesiadapiformes):The evidence for gliding behavior reconsidered." *American Journal of Physical Anthropology* **109**, 397–413.

Hamrick, M. W. (2001). "Primate origins: evolutionary change in digital ray patterning and segmentation." *Journal of Human Evolution*. **40**, 339–351.

Hansen, T. F. (1997). "Stabilizing selection and the comparative analysis of adaptation." *Evolution*. **51**:1341–1351.

Harrison, C. and A. Greensmith. (1993). Birds of the World. Doring Kindersley, inc. New York.

Hildebrand, M. and G. Gonslow. (2001). Analysis of Vertebrate Structure. 5th edition. John Wiley & Sons, Inc. New York.

Hopson, J. A. (2001) "Ecomorphology of avian and non-avian theropod phalangeal proportions: implications for the arboreal versus terrestrial origin of bird flight." In J.A. Gauthier and J.F. Gall (Eds.) New Perspectives on the Origin and Early Evolution of Birds. Proc. Int. Symp. in Honor of John H. Ostrom, New Haven, CT, 13–14 February 1999, pp. 211–235. New Haven, CT: Peabody Museum of Natural History, Yale University.

Jolly, C.J. (1967). "The evolution of the baboons". In: Vagborg E. (Ed.) The Baboon in Medical Research, vol. **2**:23–50. University of Texas Press, Austin.

Kambic, R. (2008). "Multivariate analysis of avian and non-avian theropod pedal phalanges." MS thesis, Montana State University. Bozeman, Montana.

Kirk, E. C., P. Lemelin, M.W. Hamrick D.M. Boyer, and J.I. Bloch. (2008) "Intrinsic hand proportions of euarchontans and other mammals: implications for the locomotor behavior of plesiadapiforms." *Journal of Human Evolution.* **55**: 278–299.

Lambe, L M. (1901). "On *Dryptosaurus incrassatus* (Cope) from the Edmonton Series of the North West Territory." *Contributions in Canadian Paleontology,* **1**: pp. 1-27. Geological Survey of Canada.

Lesmeister, D. B., J.J. Millspaugh, M.E. Gompper, & T.W. Mong. (2010). "Eastern spotted skunk (*Spilogale putorius*) survival and cause-specific mortality in the Ouachita Mountains, Arkansas." *The American Midland Naturalist*. **164**(1), 52–60.

Lloveras, L., M. Moreno-García, J. Nadal, J. Zilhão. (2011). "Who brought in the rabbits? Taphonomical analysis of Mousterian and Solutrean leporid accumulations from Gruta do Caldeirão (Tomar, Portugal)." *Journal of Archaeological Science*, **38**(9), 2434-2449.

Madsen, J. H., Jr. (1976). "*Allosaurus fragilis*: a revised osteology." *Utah Geological and Mineral Survey Bulletin.* **109**:1-163.

Makovicky, P., D. Li, K.Q. Gao, M. Lewin, G. Erickson, and M. Norell. (2010). "A giant ornithomimosaur from the Early Cretaceous of China." *Proceedings of the Royal Society B.* **277** (1679): 191-198

Maddison, W. (2000). "Testing character correlation using pairwise comparisons on a phylogeny." *Journal of Theoretical Biology* **202**, pp. 195-204.

Marchesi, L., P. Pedrini, and F. Sergio. (2002). "Biases associated with diet study methods in the eurasian eagle-owl." J*ournal of Raptor Research* **36**(1):11-16.

Mayr, G. (2005). "A new cypselomorph bird from the middle Eocene of Germany and the early diversification of avian aerial insectivores." *The Condor*, **107**(2), 342-352.

Morschhauser, E.M., D.J. Varricchio, C. Gao, J. Liu, Z. Wang, X. Cheng, and Q. Meng. (2009). "Anatomy of the early Cretaceous bird *Rapaxavis pani*, a new species from Liaoning province, China." *Journal of Vertebrate Paleontology* **29**:545-554

Naish, D. (2000). "Theropod dinosaurs in the trees: a historical review of arboreal habits amongst nonavian theropods." *Archaeopteryx*. **18**: 35–41.

Nowak, R.M. (1999). Walker's Mammals of the World, sixth ed. The Johns Hopkins University Press, Baltimore.

Nyakatura, J. and M. Fischer. (2011). "Functional morphology of the muscular sling at the pectoral girdle in tree sloths: convergent morphological solutions to new functional demands?" *Journal of Anatomy* **219**(3):360-374.

Osborn, H.F. (1916). "Skeletal adaptations of *Ornitholestes*, *Struthiomimus*, *Tyrannosaurus*." *Bulletin of the American Museum of Natural History* **35**: 733-771

Ostrom, J. H. (1969). "Osteology of *Deinonychus antirrhopus*, an unusual theropod from the Lower Cretaceous of Montana." *Peabody Museum Bulletin* **30**:1-165.

Perelman, P., J, W.E. Johnson, C. Roos, H.N. Seuánez, J.E. Horvath, M.A. Moreira, B. Kessing et al. (2011). "A Molecular Phylogeny of Living Primates." *PLoS Genetics*, *7*(3): e1001342.

Patel B.A., R.L. Susman, J.B. Rossie, and A. Hill (2009). "Terrestrial adaptations in the hands of *Equatorius africanus* revisited. *Journal of Human Evolution* **57**: 763-772.

Pinto, G., D. L. Mahler, L. J. Harmon, and J. B. Losos. (2008). "Testing the island effect in adaptive radiation: rates and patterns of morphological diversification in Caribbean and mainland Anolis lizards." *Proceedings of the Royal Society B.* **275**: 2749-2757.

Pyenson, N. and S. Sponberg. (2011) "Reconstructing body size in extinct crown Cetacea (Neoceti) using allometry, phylogenetic methods and tests from the fossil record." *Journal of Mammalian Evolution* **18**(4): 269-288.

Ricklefs RE, Starck JM (1996) "Applications of phylogenetically independent contrasts: a mixed progress report." *Oikos.* **77**: 167–172.

Salton J.A, and F.S. Szalay (2004). "The tarsal complex of Afro-Malagasy Tenrecoidea: a search for phylogenetically meaningful characters." *Journal of Mammalian Evolution* **11**, 73–104.

Sanchez, A. and A. Berta (2010). "The comparative anatomy and evolution of the odontocete flipper." *Marine Mammal Science*, **26**(1): 140-160.

Sereno, P. (1999). “The evolution of dinosaurs.” *Science* **284**:2137-2147.

Sereno, P. C. (1993.) “The pectoral girdle and forelimb of the basal theropod *Herrerasaurus ischigualastensis*.” *Journal of Vertebrate Paleontology.* **13**:425-450.

Smith, N. (2011) “Taxonomic revision and phylogenetic analysis of the flightless Mancallinae (Aves, Pan-Alcidae).” *ZooKeys* **91**:1-116.

Turner, A. H., D. Pol, J.A. Clarke, G.M. Erickson, and M.A. Norell (2007). “A basal dromaeosaurid and size evolution preceding avian flight.” *Science*, **317**(5843): 1378-1381.

Varricchio, D. J. (2001). “Late Cretaceous oviraptorosaur (Theropoda) dinosaurs of Montana”, pp. 42- 57. In D. Tanke and K. Carpenter (eds). Mesozoic Vertebrate Life. Indiana University Press. Bloomington, Indiana.

Witmer, L. (2002). The debate on avian ancestry: phylogeny, function, and fossils.” pp. 3–30 in L. M. Chiappe & L.M.Witmer (eds.) Mesozoic Birds: Above the Heads of Dinosaurs. University of California Press, Berkeley.

Xu, X., Z. Zhou, and X. Wang. (2000). “The smallest known non-avian theropod dinosaur.” *Nature*, **408**(6813): 705-708.

Xu, X., Z. Zhou, X. Wang, X. Kuang, F. Zhang, and X. Du. (2003). “Four-winged dinosaurs from China.” *Nature*, **421**(6921):335-340.

Xu, X., J. M. Clark, J. Mo, J. Choiniere, C.A. Forster, G.M. Erickson, D.W.E. Hone, C. Sullivan, D.A. Eberth, S. Nesbitt, Q. Zhao, R. Hernandez, C.-k. Jia, F.-l. Han, and Y. Guo. (2009). “A Jurassic ceratosaur from China helps clarify avian digital homologies.” *Nature* **459**:940-944.

Youlatos, D. and J. Meldrum (2011). “Locomotor diversification in New-World monkeys: running, climbing, or clawing along evolutionary branches.” Anatomical Record. **294**: 1991–2012.

Zanno, L. E. (2006). “The pectoral girdle and forelimb of the primitive therizinosauroid *Falcarius utahensis* (Theropoda, Maniraptora): analyzing evolutionary trends within Therizinosauroidea.” *Journal of Vertebrate Paleontology* **26**:636-650.

Zhang, F.C., Z. Zhou, X. Xu, and X. Wang. (2002). “A juvenile coelurosaurian theropod from China indicates arboreal habits. *Naturwissenschaften* **89**: 394–398.

Zhou Z. (2004). “The origin and early evolution of birds: discoveries, disputes, and perspectives from fossil evidence.” *Naturwissenschaften* **91**: 455–471.

APPENDICES

APPENDIX A

TREE USED TO MODEL PRIMATE MANUAL INTRADIGITAL PROPORTIONS

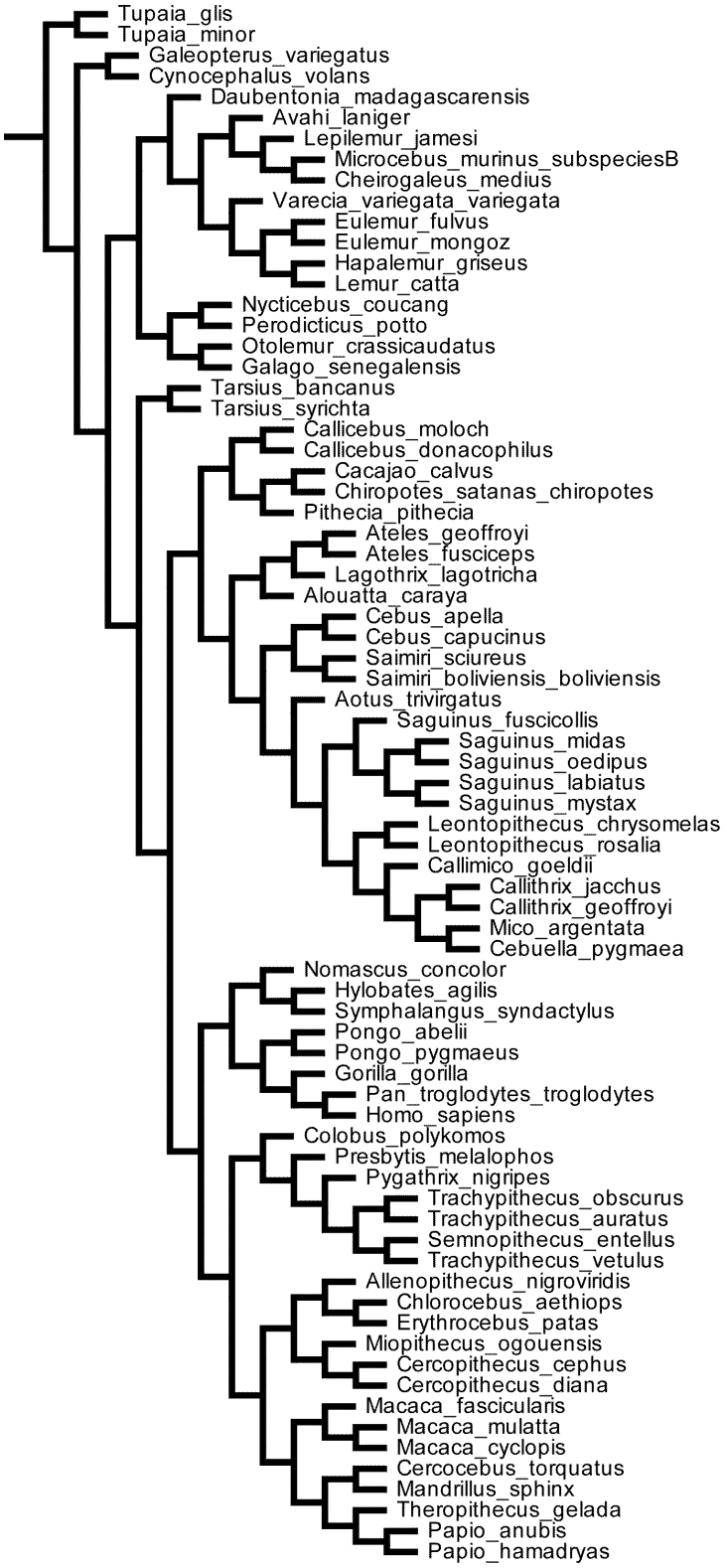
Tupaia_glis
Tupaia_minor
Galeopterus_variegatus
Cynocephalus_volans
Daubentonia_madagascarensis
Avahi_laniger
Lepilemur_jamesi
Microcebus_murinus_subspeciesB
Cheirogaleus_medius
Varecia_variegata_variegata
Eulemur_fulvus
Eulemur_mongoz
Hapalemur_griseus
Lemur_catta
Nycticebus_coucang
Perodicticus_potto
Otolemur_crassicaudatus
Galago_senegalensis
Tarsius_bancanus
Tarsius_syrichta
Callicebus_moloch
Callicebus_donacophilus
Cacajao_calvus
Chiropotes_satanas_chiropotes
Pithecia_pithecia
Ateles_geoffroyi
Ateles_fusciceps
Lagothrix_lagotricha
Alouatta_caraya
Cebus_apella
Cebus_capucinus
Saimiri_sciureus
Saimiri_boliviensis_boliviensis
Aotus_trivirgatus
Saguinus_fuscicollis
Saguinus_midas
Saguinus_oedipus
Saguinus_labiatus
Saguinus_mystax
Leontopithecus_chrysomelas
Leontopithecus_rosalia
Callimico_goeldii
Callithrix_jacchus
Callithrix_geoffroyi
Mico_argentata
Cebuella_pygmaea
Nomascus_concolor
Hylobates_agilis
Symphalangus_syndactylus
Pongo_abelii
Pongo_pygmaeus
Gorilla_gorilla
Pan_troglodytes_troglodytes
Homo_sapiens
Colobus_polykomos
Presbytis_melalophos
Pygathrix_nigripes
Trachypithecus_obscurus
Trachypithecus_auratus
Semnopithecus_entellus
Trachypithecus_vetulus
Allenopithecus_nigroviridis
Chlorocebus_aethiops
Erythrocebus_patas
Miopithecus_ogouensis
Cercopithecus_cephus
Cercopithecus_diana
Macaca_fascicularis
Macaca_mulatta
Macaca_cyclopis
Cercocebus_torquatus
Mandrillus_sphinx
Theropithecus_gelada
Papio_anubis
Papio_hamadryas

APPENDIX B

TREE USED TO MODEL BIRD PEDAL PHALANGEAL PROPORTIONS

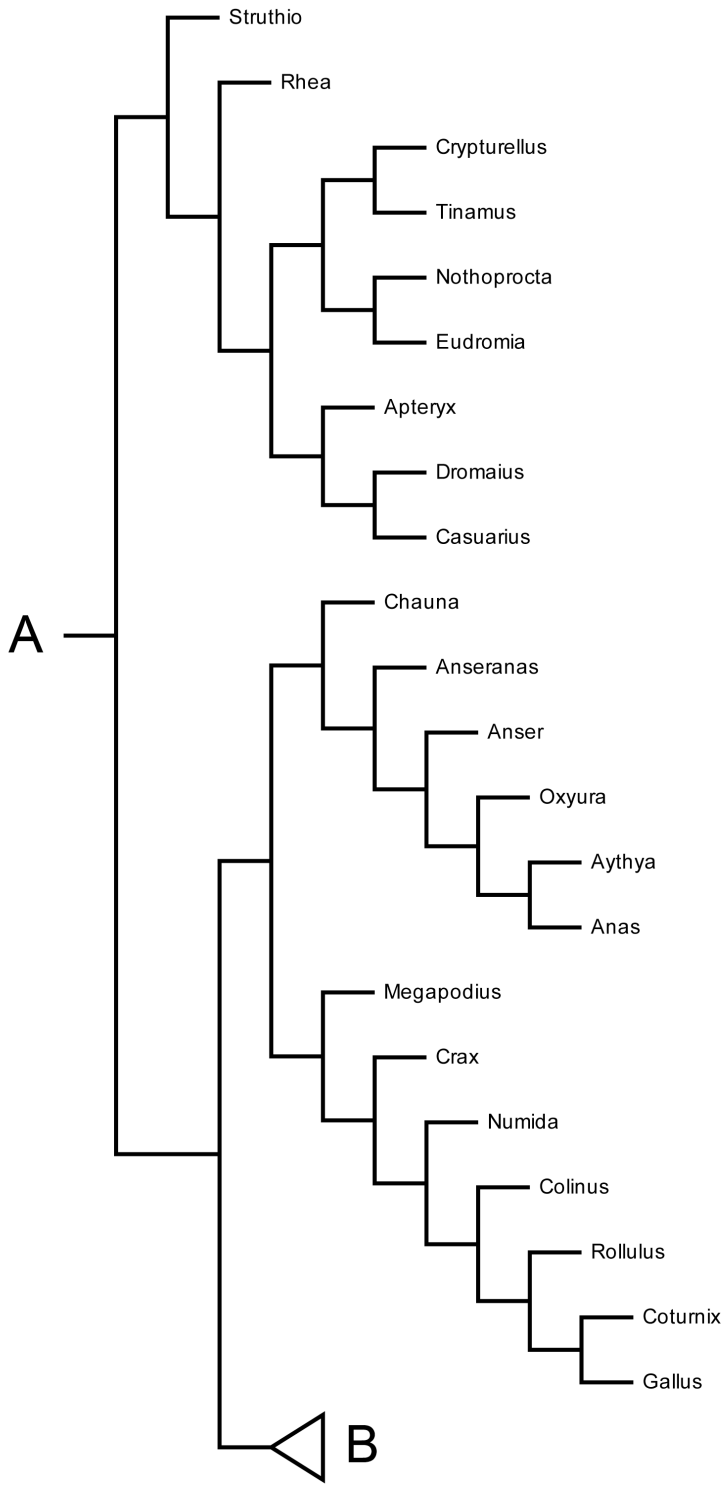
Struthio
Rhea
Crypturellus
Tinamus
Nothoprocta
Eudromia
Apteryx
Dromaius
Casuarius
A
Chauna
Anseranas
Anser
Oxyura
Aythya
Anas
Megapodius
Crax
Numida
Colinus
Rollulus
Coturnix
Gallus
B

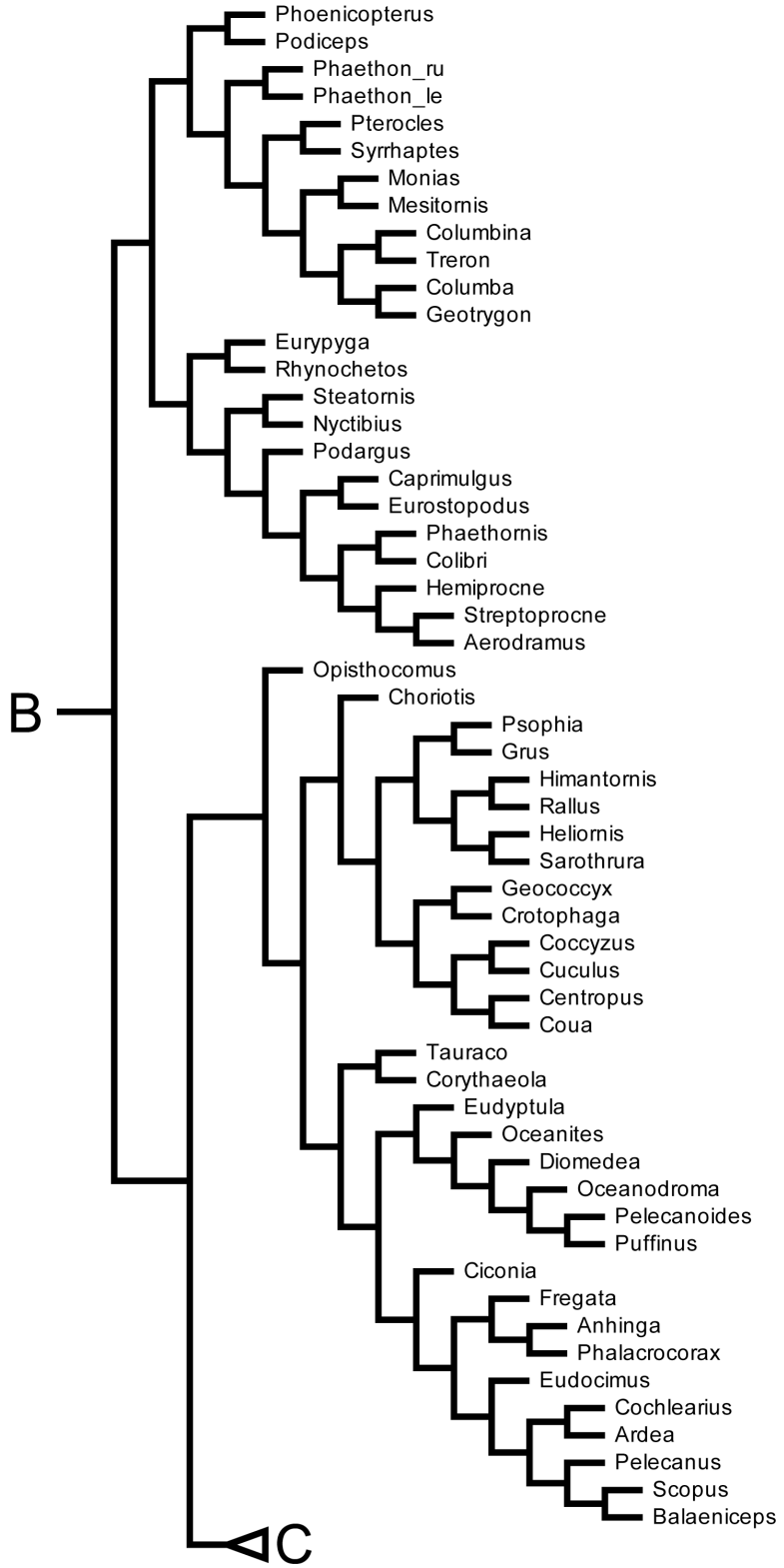
Phoenicopterus
Podiceps
Phaethon_ru
Phaethon_le
Pterocles
Syrrhaptes
Monias
Mesitornis
Columbina
Treron
Columba
Geotrygon
Eurypyga
Rhynochetos
Steatornis
Nyctibius
Podargus
Caprimulgus
Eurostopodus
Phaethornis
Colibri
Hemiprocne
Streptoprocne
Aerodramus
Opisthocomus
Choriotis
Psophia
Grus
Himantornis
Rallus
Heliornis
Sarothrura
Geococcyx
Crotophaga
Coccyzus
Cuculus
Centropus
Coua
Tauraco
Corythaeola
Eudyptula
Oceanites
Diomedea
Oceanodroma
Pelecanoides
Puffinus
Ciconia
Fregata
Anhinga
Phalacrocorax
Eudocimus
Cochlearius
Ardea
Pelecanus
Scopus
Balaeniceps
B
C

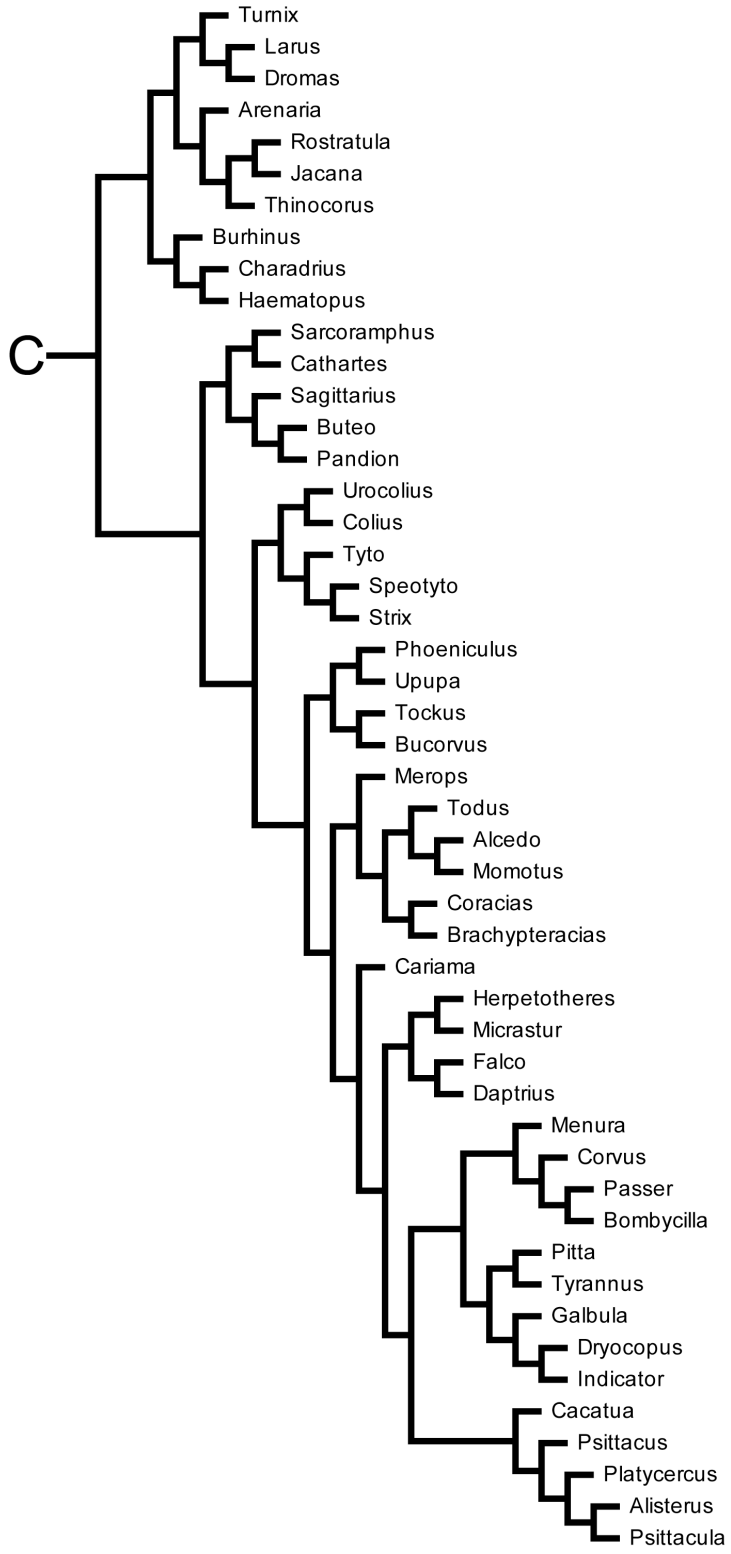
C
Turnix
Larus
Dromas
Arenaria
Rostratula
Jacana
Thinocorus
Burhinus
Charadrius
Haematopus
Sarcoramphus
Cathartes
Sagittarius
Buteo
Pandion
Urocolius
Colius
Tyto
Speotyto
Strix
Phoeniculus
Upupa
Tockus
Bucorvus
Merops
Todus
Alcedo
Momotus
Coracias
Brachypteracias
Cariama
Herpetotheres
Micrastur
Falco
Daptrius
Menura
Corvus
Passer
Bombycilla
Pitta
Tyrannus
Galbula
Dryocopus
Indicator
Cacatua
Psittacus
Platycercus
Alisterus
Psittacula

APPENDIX C

TREE USED IN MODEL FITTING OF THEROPOD MANUAL PROPORTIONS

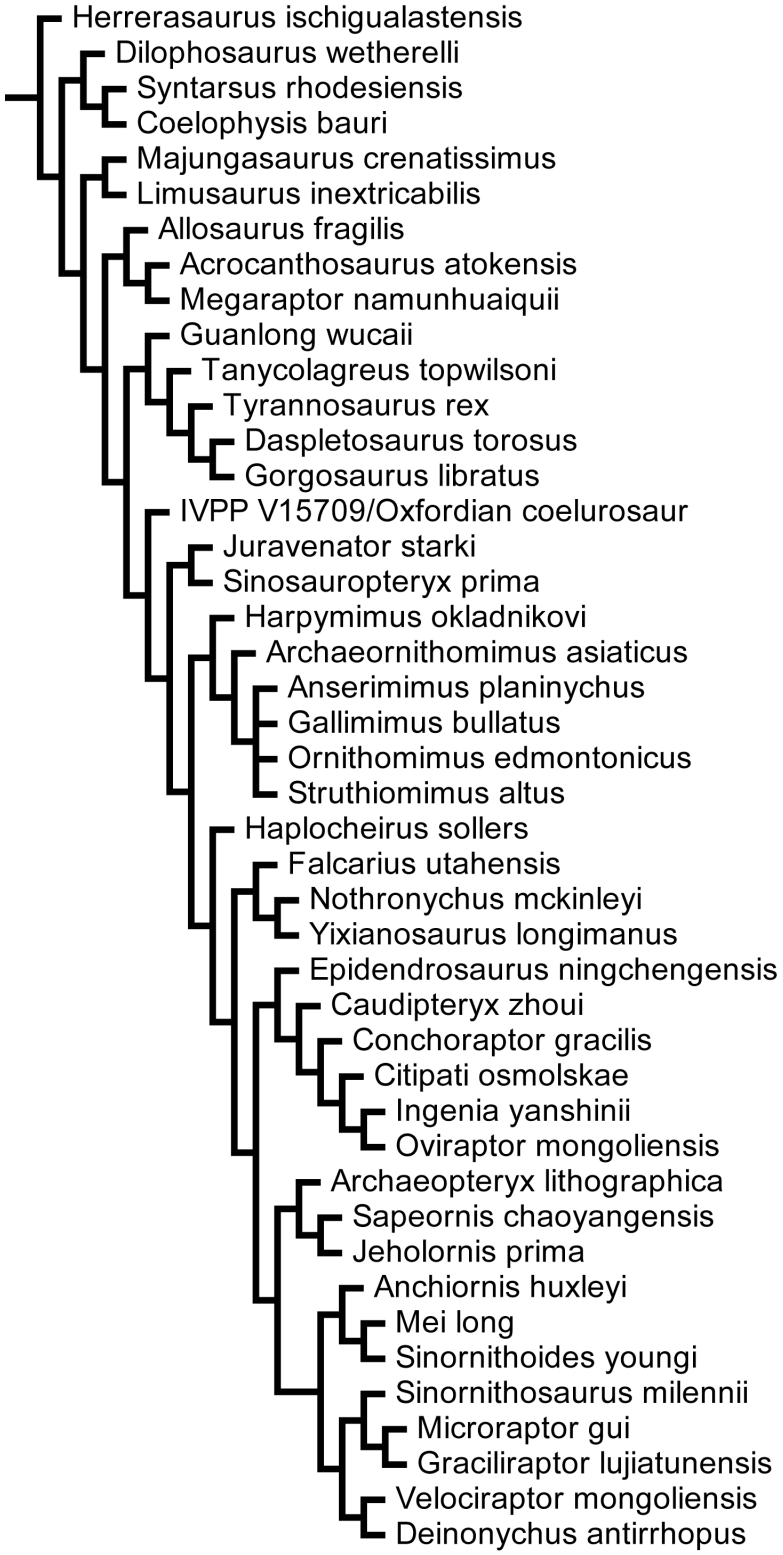
Herrerasaurus ischigualastensis
Dilophosaurus wetherelli
Syntarsus rhodesiensis
Coelophysis bauri
Majungasaurus crenatissimus
Limusaurus inextricabilis
Allosaurus fragilis
Acrocanthosaurus atokensis
Megaraptor namunhuaiquii
Guanlong wucaii
Tanycolagreus topwilsoni
Tyrannosaurus rex
Daspletosaurus torosus
Gorgosaurus libratus
IVPP V15709/Oxfordian coelurosaur
Juravenator starki
Sinosauropteryx prima
Harpymimus okladnikovi
Archaeornithomimus asiaticus
Anserimimus planinychus
Gallimimus bullatus
Ornithomimus edmontonicus
Struthiomimus altus
Haplocheirus sollers
Falcarius utahensis
Nothronychus mckinleyi
Yixianosaurus longimanus
Epidendrosaurus ningchengensis
Caudipteryx zhoui
Conchoraptor gracilis
Citipati osmolskae
Ingenia yanshinii
Oviraptor mongoliensis
Archaeopteryx lithographica
Sapeornis chaoyangensis
Jeholornis prima
Anchiornis huxleyi
Mei long
Sinornithoides youngi
Sinornithosaurus milennii
Microraptor gui
Graciliraptor lujiatunensis
Velociraptor mongoliensis
Deinonychus antirrhopus

APPENDIX D

TREE USED IN MODEL FITTING OF THEROPOD PEDAL PROPORTIONS

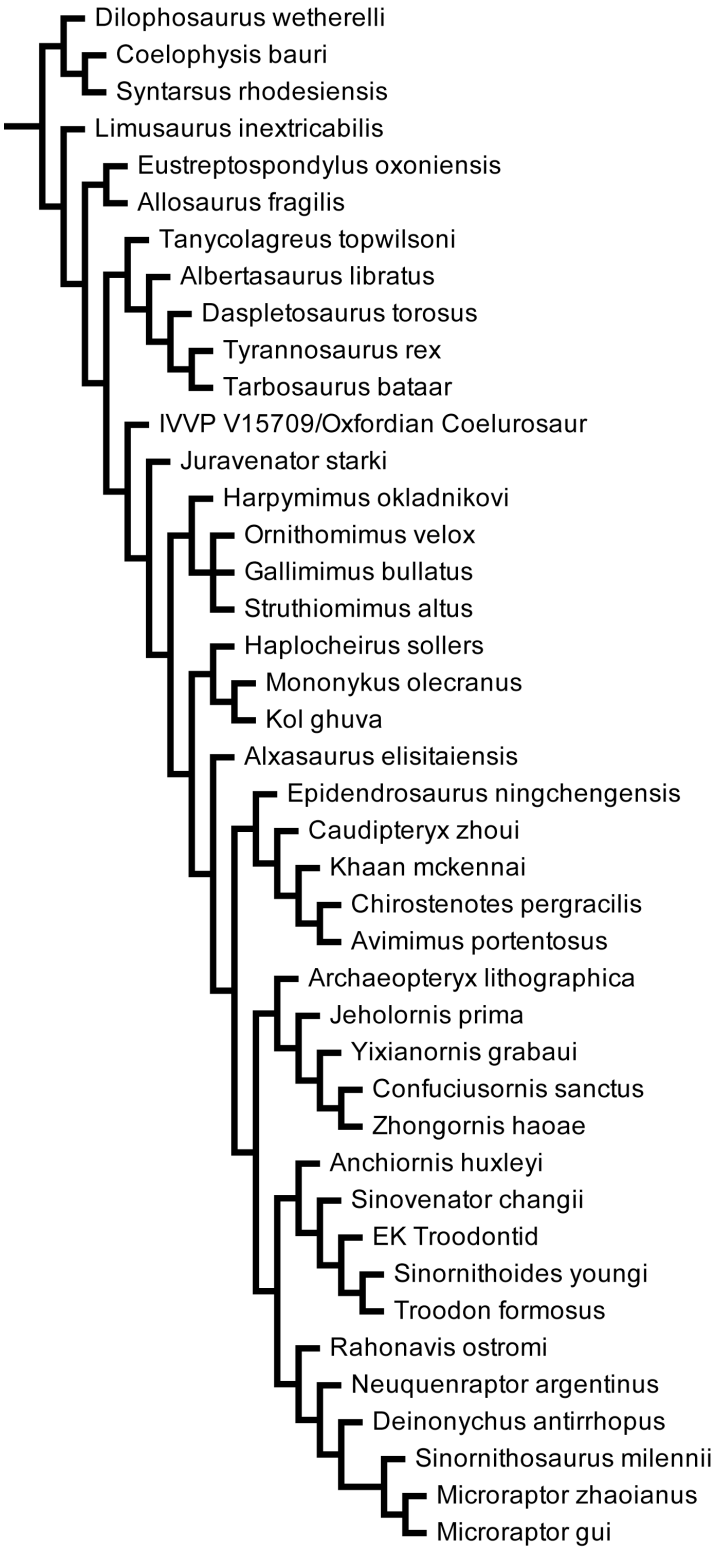
Dilophosaurus wetherelli
Coelophysis bauri
Syntarsus rhodesiensis
Limusaurus inextricabilis
Eustreptospondylus oxoniensis
Allosaurus fragilis
Tanycolagreus topwilsoni
Albertasaurus libratus
Daspletosaurus torosus
Tyrannosaurus rex
Tarbosaurus bataar
IVVP V15709/Oxfordian Coelurosaur
Juravenator starki
Harpymimus okladnikovi
Ornithomimus velox
Gallimimus bullatus
Struthiomimus altus
Haplocheirus sollers
Mononykus olecranus
Kol ghuva
Alxasaurus elisitaiensis
Epidendrosaurus ningchengensis
Caudipteryx zhoui
Khaan mckennai
Chirostenotes pergracilis
Avimimus portentosus
Archaeopteryx lithographica
Jeholornis prima
Yixianornis grabaui
Confuciusornis sanctus
Zhongornis haoae
Anchiornis huxleyi
Sinovenator changii
EK Troodontid
Sinornithoides youngi
Troodon formosus
Rahonavis ostromi
Neuquenraptor argentinus
Deinonychus antirrhopus
Sinornithosaurus milennii
Microraptor zhaoianus
Microraptor gui

APPENDIX E.

PRIMATE MANUAL INTRADIGITAL DATA AND BEHAVIORAL REGIMES

MCper=mean metacarpal%, MPPper=mean manual proximal phalangeal %, MIPper=mean intermediate phalangeal %, PHOU2=behavioral regime assignments for model PHOU2 (0=terrestrial, 1=arboreal), PHOU3=behavioral regime assignments or model PHOU3 (0=terrestrial, 1=arboreal, 2=vertical clinging)

Taxon	**MCper**	**MPPper**	**MIPper**	***PHOU2***	***PHOU3***
Macaca_mulatta	0.426716141	0.354359926	0.218923933	1	1
Macaca_cyclopis	0.440894569	0.333865815	0.225239617	1	1
Macaca_fascicularis	0.444162437	0.345177665	0.210659898	1	1
Papio_anubis	0.53372434	0.279569892	0.186705767	0	0
Papio_hamadryas	0.51810585	0.299442897	0.182451253	0	0
Theropithecus_gelada	0.596843615	0.261119082	0.142037303	0	0
Cercocebus_torquatus	0.465020576	0.326474623	0.208504801	1	1
Mandrillus_sphinx	0.511146497	0.292993631	0.195859873	0	0
Cercopithecus_cephus	0.438333333	0.336666667	0.225	1	1
Cercopithecus_diana	0.410183876	0.345120226	0.244695898	1	1
Miopithecus_ogouensis	0.411057692	0.338942308	0.25	1	1
Chlorocebus_aethiops	0.436928702	0.321755027	0.241316271	1	1
Erythrocebus_patas	0.549768519	0.280092593	0.170138889	0	0
Allenopithecus_nigroviridis	0.477927063	0.3378119	0.184261036	0	0
Trachypithecus_obscurus	0.430555556	0.344907407	0.224537037	1	1
Trachypithecus_auratus	0.450160772	0.32261522	0.227224009	1	1
Semnopithecus_entellus	0.430678466	0.327433628	0.241887906	1	1
Trachypithecus_vetulus	0.440652819	0.332344214	0.227002967	1	1
Pygathrix_nigripes	0.422163588	0.335971856	0.241864556	1	1
Presbytis_melalophos	0.410617551	0.344528711	0.244853738	1	1
Colobus_polykomos	0.416500994	0.337972167	0.245526839	1	1
Hylobates_agilis	0.412587413	0.347552448	0.23986014	1	1
Symphalangus_syndactylus	0.449796472	0.34531886	0.204884668	1	1
Nomascus_concolor	0.439425051	0.331279945	0.229295003	1	1
Pan_troglodytes_troglodytes	0.468108708	0.321686079	0.210205214	1	1
Homo_sapiens	0.450966356	0.326413744	0.2226199	0	0
Gorilla_gorilla	0.487957611	0.303468208	0.208574181	0	0
Pongo_abelii	0.433707865	0.353932584	0.212359551	1	1
Pongo_pygmaeus	0.450941526	0.335480674	0.2135778	1	1
Callithrix_jacchus	0.408450704	0.35915493	0.232394366	1	2
Callithrix_geoffroyi	0.435736677	0.34169279	0.222570533	1	2
Mico_argentata	0.411564626	0.343537415	0.244897959	1	2
Cebuella_pygmaea	0.392156863	0.343137255	0.264705882	1	2
Callimico_goeldii	0.43454039	0.337047354	0.228412256	1	2

Leontopithecus_chrysomelas	0.457038391	0.327239488	0.215722121	1	2
Leontopithecus_rosalia	0.465725806	0.322580645	0.211693548	1	2
Saguinus_midas	0.421538462	0.363076923	0.215384615	1	2
Saguinus_oedipus	0.438438438	0.339339339	0.222222222	1	2
Saguinus_labiatus	0.424698795	0.355421687	0.219879518	1	2
Saguinus_mystax	0.446327684	0.336158192	0.217514124	1	2
Saguinus_fuscicollis	0.434782609	0.341137124	0.224080268	1	2
Aotus_trivirgatus	0.414529915	0.344017094	0.241452991	1	1
Cebus_apella	0.430426716	0.33580705	0.233766234	1	1
Cebus_capucinus	0.401851852	0.353703704	0.244444444	1	1
Saimiri_sciureus	0.397297297	0.351351351	0.251351351	1	2
Saimiri_boliviensis_boliviens	0.404891304	0.345108696	0.25	1	2
Ateles_geoffroyi	0.426712923	0.333911535	0.239375542	1	1
Ateles_fusciceps	0.432098765	0.335097002	0.232804233	1	1
Lagothrix_lagotricha	0.392419175	0.372352285	0.23522854	1	1
Alouatta_caraya	0.3820059	0.377581121	0.240412979	1	1
Callicebus_moloch	0.386117137	0.351409978	0.262472885	1	1
Callicebus_donacophilus	0.372141372	0.365904366	0.261954262	1	1
Cacajao_calvus	0.369565217	0.369565217	0.260869565	1	1
Chiropotes_satanas_chiropote	0.387337058	0.357541899	0.255121043	1	2
Pithecia_pithecia	0.357638889	0.371527778	0.270833333	1	2
Tarsius_bancanus	0.314363144	0.398373984	0.287262873	1	2
Tarsius_syrichta	0.344512195	0.381097561	0.274390244	1	2
Lepilemur_jamesi	0.383297645	0.353319058	0.263383298	1	2
Microcebus_murinus_subspec	0.383561644	0.342465753	0.273972603	1	2
Cheirogaleus_medius	0.351464435	0.393305439	0.255230126	1	2
Avahi_laniger	0.395833333	0.33125	0.272916667	1	2
Eulemur_fulvus	0.414762742	0.360281195	0.224956063	1	1
Eulemur_mongoz	0.395927602	0.346153846	0.257918552	1	1
Hapalemur_griseus	0.404199475	0.362204724	0.233595801	1	2
Lemur_catta	0.405152225	0.365339578	0.229508197	1	1
Varecia_variegata_variegata	0.365638767	0.37298091	0.261380323	1	2
Daubentonia_madagascarensi	0.219979818	0.456104945	0.323915237	1	1
Nycticebus_coucang	0.361111111	0.420138889	0.21875	1	1
Perodicticus_potto	0.373219373	0.438746439	0.188034188	1	1
Otolemur_crassicaudatus	0.388888889	0.391975309	0.219135802	1	1
Galago_senegalensis	0.340425532	0.391489362	0.268085106	1	2
Galeopterus_variegatus	0.403169014	0.26584507	0.330985915	1	2
Cynocephalus_volans	0.413547237	0.22459893	0.361853832	1	2
Tupaia_glis	0.526041667	0.286458333	0.1875	0	0
Tupaia_minor	0.44375	0.3	0.25625	1	1

APPENDIX F.

BIRD PEDAL INTRADIGITAL DATA

PP=proximal phalangeal%, IP=intermediate phalangeal %, DP=distal phalangeal %

TABLE S2

Taxon	PP	IP	DP
Aerodramus	0.236363636	0.181818182	0.581818182
Alcedo	0.322	0.317	0.361
Alisterus	0.364035088	0.307017544	0.328947368
Anas	0.322	0.317	0.361
Anhinga	0.331569665	0.33686067	0.331569665
Anser	0.435810811	0.298986486	0.265202703
Anseranas	0.434072345	0.297549592	0.268378063
Apteryx	0.400484274	0.311132249	0.288383477
Ardea	0.379844961	0.36627907	0.253875969
Arenaria	0.421621622	0.324324324	0.254054054
Aythya	0.434862385	0.317431193	0.247706422
Balaeniceps	0.418734491	0.322580645	0.258684864
Bombycilla	0.325888019	0.304675898	0.369436083
Brachypteracias	0.353	0.314	0.332
Bucorvus	0.47	0.26	0.27
Burhinus	0.426	0.333	0.241
Buteo	0.426	0.18	0.3945
Cacatua	0.3455	0.2775	0.377
Caprimulgus	0.398	0.311	0.291
Cariama	0.487	0.302	0.211
Casuarius	0.469	0.324	0.208
Cathartes	0.381	0.318	0.302
Centropus	0.375	0.33	0.295
Charadrius	0.391534392	0.333333333	0.275132275
Chauna	0.409617097	0.300979519	0.289403384
Choriotis	0.542429285	0.297836938	0.159733777
Ciconia	0.482804233	0.276455026	0.240740741
Coccyzus	0.335	0.301	0.3645
Cochlearius	0.35125448	0.374551971	0.274193548
Colibri	0.304347826	0.260869565	0.434782609
Colinus	0.392	0.316	0.292
Colius	0.299	0.28	0.421
Columba	0.388	0.32	0.2918
Columbina	0.402877698	0.302158273	0.294964029
Coracias	0.374015748	0.299212598	0.326771654
Corvus	0.3295	0.3125	0.358
Corythaeola	0.393280632	0.308300395	0.298418972

Coturnix	0.391705069	0.331797235	0.276497696
Coua	0.392	0.315	0.293
Crax	0.43	0.325	0.244
Crotophaga	0.371	0.309	0.32
Crypturellus	0.419	0.33	0.251
Cuculus	0.362	0.313	0.325
Daptrius	0.397	0.296	0.307
Diomedea	0.477799228	0.299227799	0.222972973
Dromaius	0.499580889	0.328583403	0.171835708
Dromas	0.494444444	0.294444444	0.211111111
Dryocopus	0.27	0.316	0.4135
Eudocimus	0.3796875	0.340625	0.2796875
Eudromia	0.447698745	0.30125523	0.251046025
Eudyptula	0.421828909	0.318584071	0.259587021
Eurostopodus	0.414634146	0.298780488	0.286585366
Eurypyga	0.409470752	0.331476323	0.259052925
Falco	0.402	0.2725	0.3255
Fregata	0.318944844	0.323741007	0.357314149
Galbula	0.380530973	0.283185841	0.336283186
Gallus	0.4115	0.308	0.28
Geococcyx	0.3795	0.339	0.282
Geotrygon	0.392	0.33	0.279
Grus	0.458	0.296	0.246
Haematopus	0.438235294	0.314705882	0.247058824
Heliornis	0.404844291	0.297577855	0.297577855
Hemiprocne	0.303571429	0.25	0.446428571
Herpetotheres	0.379227053	0.282608696	0.338164251
Himantornis	0.424164524	0.300771208	0.275064267
Indicator	0.324675325	0.324675325	0.350649351
Jacana	0.455	0.308	0.236
Larus	0.471728595	0.295638126	0.232633279
Megapodius	0.449197861	0.323529412	0.227272727
Menura	0.276	0.332	0.392
Merops	0.355	0.302	0.343
Mesitornis	0.380165289	0.318181818	0.301652893
Micrastur	0.388714734	0.253918495	0.357366771
Momotus	0.360215054	0.311827957	0.327956989
Monias	0.372881356	0.322033898	0.305084746
Nothoprocta	0.42962963	0.322222222	0.248148148
Numida	0.426	0.319	0.256
Nyctibius_gr	0.352173913	0.313043478	0.334782609
Oceanites	0.555555556	0.243589744	0.200854701

Oceanodroma	0.448377581	0.297935103	0.253687316
Opisthocomus	0.337	0.339	0.324
Oxyura	0.431818182	0.308712121	0.259469697
Pandion	0.3545	0.1345	0.511
Passer	0.305732484	0.331210191	0.363057325
Pelecanoides	0.421875	0.2734375	0.3046875
Pelecanus	0.442424242	0.337662338	0.21991342
Phaethon_le	0.37704918	0.301639344	0.321311475
Phaethon_ru	0.304109589	0.342465753	0.353424658
Phaethornis	0.387096774	0.225806452	0.387096774
Phalacrocorax	0.38358209	0.328358209	0.288059701
Phoenicopterus	0.603244838	0.259587021	0.137168142
Phoeniculus	0.300492611	0.320197044	0.379310345
Pitta	0.321	0.346	0.333
Platycercus	0.346534653	0.287128713	0.366336634
Podargus	0.384615385	0.323607427	0.291777188
Podiceps	0.401140684	0.309885932	0.288973384
Psittacula	0.342391304	0.293478261	0.364130435
Psittacus	0.335	0.274	0.391
Psophia	0.392	0.292	0.316
Pterocles	0.479	0.315	0.206
Puffinus	0.479302832	0.294117647	0.226579521
Rallus	0.417827298	0.311977716	0.270194986
Rhea	0.526	0.322	0.153
Rhynochetos	0.395927602	0.337104072	0.266968326
Rollulus	0.393728223	0.341463415	0.264808362
Rostratula	0.396174863	0.327868852	0.275956284
Sagittarius	0.516	0.2595	0.2245
Sarcoramphus	0.386819484	0.297994269	0.315186246
Sarothrura	0.433035714	0.325892857	0.241071429
Scopus	0.440251572	0.314465409	0.245283019
Speotyto	0.252	0.31	0.438
Steatornis	0.348	0.276	0.375
Streptoprocne	0.303	0.203	0.494
Strix	0.229	0.305	0.467
Struthio	0.519	0.302	0.179
Syrrhaptes	0.501	0.292	0.207
Tauraco	0.369666667	0.316666667	0.313666667
Thinocorus	0.395348837	0.31627907	0.288372093
Tinamus	0.442	0.331	0.227
Tockus	0.3905	0.284	0.326
Todus	0.293785311	0.338983051	0.367231638

Treron	0.371	0.33	0.299
Turnix	0.453	0.286	0.261
Tyrannus	0.321	0.283	0.395
Tyto	0.234	0.357	0.409
Upupa	0.379562044	0.313868613	0.306569343
Urocolius	0.24	0.333	0.427

APPENDIX G.

BEHAVIORAL REGIME ASSIGNMENTS FOR EXTANT BIRD MODELS

BFOU2 - (0=terrestrial, 1=arboreal or predatory), BFOU3 - (0=terrestrial, 1=arboreal grasping/perching, 2=vertical clinging and raptors), BFOU4 - (0=terrestrial, 1=arboreal grasping/perching, 2=vertical clinging, 3=raptors), BFOU5 - (0=terrestrial, 1=arboreal, 2=vertical clinging/accipitrid/strigiform, 3=falconid), BFOU6 - (0=terrestrial/falconid, 1=arboreal grasping/perching, 2=vertical clinging/accipitrid/strigiform)

Taxon	***BFOU2***	***BFOU3***	***BFOU4***	***BFOU5***	***BFOU6***
Aerodramus	1	2	2	2	2
Alcedo	1	1	1	1	1
Alisterus	1	1	1	1	1
Anas	0	0	0	0	0
Anhinga	0	0	0	0	0
Anser	0	0	0	0	0
Anseranas	0	0	0	0	0
Apteryx	0	0	0	0	0
Ardea	0	0	0	0	0
Arenaria	0	0	0	0	0
Aythya	0	0	0	0	0
Balaeniceps	0	0	0	0	0
Bombycilla	1	1	1	1	1
Brachypteracias	1	1	1	1	1
Bucorvus	0	0	0	0	0
Burhinus	0	0	0	0	0
Buteo	1	2	3	2	2
Cacatua	1	1	1	1	1
Caprimulgus	0	0	0	0	0
Cariama	0	0	0	0	0
Casuarius	0	0	0	0	0
Cathartes	0	0	0	0	0
Centropus	1	1	1	1	1
Charadrius	0	0	0	0	0
Chauna	0	0	0	0	0
Choriotis	0	0	0	0	0
Ciconia	0	0	0	0	0
Coccyzus	1	1	1	1	1
Cochlearius	0	0	0	0	0
Colibri	1	1	1	1	1
Colinus	0	0	0	0	0
Colius	1	1	1	1	1
Columba	0	0	0	0	0

Columbina	0	0	0	0	0
Coracias	1	1	1	1	1
Corvus	1	1	1	1	1
Corythaeola	1	1	1	1	1
Coturnix	0	0	0	0	0
Coua	0	0	0	0	0
Crax	0	0	0	0	0
Crotophaga	1	1	1	1	1
Crypturellus	0	0	0	0	0
Cuculus	1	1	1	1	1
Daptrius	1	2	3	3	0
Diomedea	0	0	0	0	0
Dromaius	0	0	0	0	0
Dromas	0	0	0	0	0
Dryocopus	1	2	2	2	2
Eudocimus	0	0	0	0	0
Eudromia	0	0	0	0	0
Eudyptula	0	0	0	0	0
Eurostopodus	0	0	0	0	0
Eurypyga	0	0	0	0	0
Falco	1	2	3	3	0
Fregata	0	0	0	0	0
Galbula	1	1	1	1	1
Gallus	0	0	0	0	0
Geococcyx	0	0	0	0	0
Geotrygon	0	0	0	0	0
Grus	0	0	0	0	0
Haematopus	0	0	0	0	0
Heliornis	0	0	0	0	0
Hemiprocne	1	1	1	1	1
Herpetotheres	1	2	3	3	0
Himantornis	0	0	0	0	0
Indicator	1	1	1	1	1
Jacana	0	0	0	0	0
Larus	0	0	0	0	0
Megapodius	0	0	0	0	0
Menura	0	0	0	0	0
Merops	1	1	1	1	1
Mesitornis	0	0	0	0	0
Micrastur	1	2	3	3	0
Momotus	1	1	1	1	1
Monias	0	0	0	0	0

Nothoprocta	0	0	0	0	0
Numida	0	0	0	0	0
Nyctibius_gr	1	1	1	1	1
Oceanites	0	0	0	0	0
Oceanodroma	0	0	0	0	0
Opisthocomus	1	1	1	1	1
Oxyura	0	0	0	0	0
Pandion	1	2	3	2	2
Passer	1	1	1	1	1
Pelecanoides	0	0	0	0	0
Pelecanus	0	0	0	0	0
Phaethon_le	0	0	0	0	0
Phaethon_ru	0	0	0	0	0
Phaethornis	1	1	1	1	1
Phalacrocorax	0	0	0	0	0
Phoenicopterus	0	0	0	0	0
Phoeniculus	1	2	2	2	2
Pitta	0	0	0	0	0
Platycercus	1	1	1	1	1
Podargus	1	1	1	1	1
Podiceps	0	0	0	0	0
Psittacula	1	1	1	1	1
Psittacus	1	1	1	1	1
Psophia	0	0	0	0	0
Pterocles	0	0	0	0	0
Puffinus	0	0	0	0	0
Rallus	0	0	0	0	0
Rhea	0	0	0	0	0
Rhynochetos	0	0	0	0	0
Rollulus	0	0	0	0	0
Rostratula	0	0	0	0	0
Sagittarius	0	0	0	0	0
Sarcoramphus	0	0	0	0	0
Sarothrura	0	0	0	0	0
Scopus	0	0	0	0	0
Speotyto	1	2	3	2	2
Steatornis	1	2	2	2	2
Streptoprocne	1	2	2	2	2
Strix	1	2	3	2	2
Struthio	0	0	0	0	0
Syrrhaptes	0	0	0	0	0

Tauraco	1	1	1	1	1
Thinocorus	0	0	0	0	0
Tinamus	0	0	0	0	0
Tockus	1	1	1	1	1
Todus	1	1	1	1	1
Treron	1	1	1	1	1
Turnix	0	0	0	0	0
Tyrannus	1	1	1	1	1
Tyto	1	2	3	2	2
Upupa	0	0	0	0	0
Urocolius	1	2	2	2	2

APPENDIX H

MESOZOIC THEROPOD MANUAL INTRADIGITAL DATA AND BEHAVIORAL REGIMES

MC=metacarpal %, PP=proximal phalangeal %, IP=intermediate phalangeal %, THOU2- (0=non-avian theropod, 1=mesozoic bird), THOU3 - (0=non-avian theropod excluding microraptorines, 1=microraptorines + mesozoic birds), THOU4 - (0=non-avian theropod excluding small bodied maniraptorans, 1=mesozoic bird, 2=small bodied non-avian maniraptorans)

Taxon	**MC**	**PP**	**IP**	***THOU2***	***THOU3***	***THOU4***
Acrocanthosaurus_atokensis	0.3625	0.31563	0.321875	0	0	0
Allosaurus_fragilis	0.38941	0.29283	0.317757	0	0	0
Anchiornis_huxleyi	0.4307	0.20896	0.360341	0	0	2
Anserimimus_planinychus	0.37245	0.25	0.377551	0	0	0
Archaeopteryx_lithographica	0.43836	0.24105	0.320592	1	1	1
Archaeornithomimus_asiaticus	0.3913	0.19565	0.413043	0	0	0
Caudipteryx_zhoui	0.4	0.25517	0.344828	0	0	0
Chonchoraptor_gracilis	0.56774	0.23613	0.196129	0	0	0
Citipati_osmolskae	0.44306	0.2667	0.290245	0	0	0
Coelophysis_bauri	0.44144	0.20946	0.349099	0	0	0
Daspletosaurus_torosus	0.46032	0.22222	0.31746	0	0	0
Deinonychus_antirrhopus	0.41374	0.24022	0.346038	0	0	0
Dilophosaurus_wetherelli	0.44118	0.29412	0.264706	0	0	0
Epidendrosaurus_ningchengensis	0.38768	0.22826	0.384058	0	0	2
Falcarius_utahensis	0.37626	0.27767	0.346076	0	0	0
Gallimimus_bullatus	0.4291	0.19776	0.373134	0	0	0
Gorgosaurus_libratus	0.40426	0.24255	0.353191	0	0	0
Graciliraptor_lujiatunensis	0.49716	0.2339	0.268939	0	1	2
Guanlong_wucaii	0.37662	0.28571	0.337662	0	0	0
Hagryphus_giganteus	0.38608	0.30063	0.313291	0	0	0
Haplocheirus_sollers	0.56405	0.31582	0.120129	0	0	0
Harpymimus_okladnikovi	0.38057	0.19838	0.421053	0	0	0
Herrerasaurus_ischigualastensi	0.44275	0.27481	0.282443	0	0	0
Ingenia_yanshinii	0.55911	0.23526	0.20563	0	0	0
IVPP V15709	0.38166	0.23336	0.384978	0	0	2
Jeholornis prima	0.49796	0.24152	0.260516	1	1	1
Juravenator_starki	0.38983	0.27119	0.338983	0	0	0
Khaan mckennai	0.42564	0.2681	0.306262	0	0	0
Majungasaurus_crenatissimus	0.52381	0.33333	0.142857	0	0	0
Megaraptor_namunhuaiquii	0.44503	0.28272	0.272251	0	0	0
Mei_long	0.38462	0.23077	0.384615	0	0	2
Microraptor_gui	0.52184	0.22668	0.251476	0	1	2
Nothronychus_graffami	0.37493	0.27084	0.354222	0	0	0

Ornithomimus_edmontonicus	0.42593	0.15741	0.416667	0	0	0
Oviraptor_philoceratops	0.46522	0.23913	0.295652	0	0	0
Sapeornis	0.49739	0.26132	0.241289	1	1	1
Sinornithoides_youngi	0.41615	0.22981	0.354037	0	0	0
Sinornithosaurus_milennii	0.48814	0.23385	0.278005	0	1	2
Sinosauropteryx_prima	0.48994	0.21422	0.295835	0	0	0
Struthiomimus_altus	0.4257	0.16867	0.405622	0	0	0
Tanycolagreus_topwilsoni	0.36652	0.29412	0.339367	0	0	0
Tyrannosaurus_rex	0.43008	0.23729	0.332627	0	0	0
Velociraptor_mongoliensis	0.39719	0.24472	0.358092	0	0	0
Yixianosaurus_longimanus	0.36458	0.26042	0.375	0	0	2

APPENDIX I

MESOZOIC THEROPOD PEDAL INTRADIGITAL DATA AND BEHAVIORAL REGIMES

PP=proximal phalangeal%, IP=intermediate phalangeal %, DP=distal phalangeal %, TFOU2 - (0=non-avian, 1=avian), TFOU3 - (0=non-paravian, 1=avian, 2=deinonychosaurian), TFOU4 - (0=non-paravian+troodontids, 1=avian, 2=dromaeosaurid)

Taxon	PP	IP	DP	*TFOU2*	*TFOU3*	*TFOU4*
Albertasaurus_libratus	0.446023	0.27841	0.275568	0	0	0
Allosaurus_fragilis	0.409473	0.33957	0.250955	0	0	0
Alxasaurus_elisitaiensis	0.454545	0.26515	0.280303	0	0	0
Anchiornis_huxleyi	0.379464	0.29018	0.330357	0	2	0
Archaeopteryx_lithographica	0.378194	0.32926	0.292549	1	1	1
Avimimus_portentosus	0.456628	0.33224	0.211129	0	0	0
Caudipteryx_zhoui	0.413793	0.32759	0.258621	0	0	0
Chirostenotes_pergracilis	0.405405	0.28108	0.313514	0	0	0
Coelophysis_bauri	0.409977	0.31519	0.274829	0	0	0
Confuciusornis_sanctus	0.373376	0.30735	0.319271	1	1	1
Daspletosaurus_torosus	0.477778	0.3	0.222222	0	0	0
Deinonychus_antirrhopus	0.447242	0.28571	0.26112	0	2	2
Dilophosaurus_wetherelli	0.416667	0.31818	0.265152	0	0	0
EK_Troodontid	0.5	0.2931	0.206897	0	2	0
Epidendrosaurus_ningchengensis	0.357143	0.28571	0.357143	0	0	0
Eustreptospondylus_oxoniensis	0.40201	0.32663	0.271357	0	0	0
IVVP V15709	0.407463	0.30474	0.287798	0	0	0
Gallimimus bullatus	0.430922	0.33688	0.232201	0	0	0
Haplocheirus_sollers	0.425861	0.28696	0.28718	0	0	0
Harpymimus_okladnikovi	0.406061	0.32727	0.266667	0	0	0
Jeholornis prima	0.378472	0.36806	0.253472	1	1	1
Juravenator_starki	0.434307	0.29562	0.270073	0	0	0
Khaan_mckennai	0.438779	0.30793	0.253288	0	0	0
Kol_ghuva	0.439024	0.31707	0.243902	0	0	0
Limusaurus_inextricabilis	0.439024	0.31707	0.243902	0	0	0
Microraptor_gui	0.395878	0.31992	0.284203	0	2	2
Microraptor_zhaoianus	0.395878	0.29976	0.247002	0	2	2
Mononykus_olecranus	0.454006	0.30861	0.237389	0	0	0
Neuquenraptor_argentinus	0.463875	0.26273	0.273399	0	2	2
Ornithomimus_velox	0.38172	0.29032	0.327957	0	0	0
Rahonavis_ostromi	0.453237	0.29976	0.247002	0	2	2
Sinornithoides_youngi	0.433962	0.31447	0.251572	0	2	0
Sinornithosaurus_milennii	0.442379	0.2974	0.260223	0	2	2
Sinovenator_changii	0.449485	0.29072	0.259794	0	2	0

Struthiomimus_altus	0.45614	0.31579	0.22807	0	0	0
Syntarsus_rhodesiensis	0.413633	0.29594	0.290432	0	0	0
Tanycolagreus_topwilsoni	0.431953	0.32544	0.242604	0	0	0
Tarbosaurus_bataar	0.416667	0.31818	0.265152	0	0	0
Troodon_formosus	0.450512	0.28123	0.268259	0	2	0
Tyrannosaurus_rex	0.437908	0.2963	0.265795	0	0	0
Yixianornis_grabaui	0.403509	0.30526	0.291228	1	1	1
Zhongornis_haoae	0.359551	0.29213	0.348315	1	1	1